U.PORTO
FEUP FACULDADE DE ENGENHARIA
UNIVERSIDADE DO PORTO

FUNCTIONALISATION OF BRAIDED STRUCTURES FOR TENDON AND LIGAMENT REPAIR

DANIEL BARROS DA SILVA
DISSERTAÇÃO DE MESTRADO APRESENTADA
À FACULDADE DE ENGENHARIA DA UNIVERSIDADE DO PORTO EM 31 DE MARÇO DE 2022

ORIENTADORA: MARIA ASCENSÃO LOPES

Departamento de Engenharia Metalúrgica e de Materiais da Faculdade de Engenharia da Universidade do Porto

COORIENTADOR: RAÚL FANGUEIRO

Centro de Ciência e Tecnologia Têxtil da Escola de Engenharia da Universidade do Minho

U.PORTO
FEUP FACULDADE DE ENGENHARIA
UNIVERSIDADE DO PORTO

CANDIDATO		*Código*
TÍTULO		
DATA	__ de _____ de _____	
LOCAL	Faculdade de Engenharia da Universidade do Porto – Sala _____ - __:__h	
JÚRI	*Presidente*	DEMM/FEUP
	Arguente	DEM/FEUP
	Orientador	DEMM/FEUP

Abstract

Tendon and ligament injuries are very frequent and often quite debilitating to the quality of life of the worldwide population, leading some professionals whose career is directly related to their physical health to early retirement. The main goal of this work was to compare different methods of functionalisation of braided structures for tendon and ligament repair to promote cell adhesion and proliferation without compromising the mechanical performance of the medical device, and therefore increase its long term success. The functionalisation methods were based on NH_3 plasma treatment and an O_2 plasma treatment followed by immersion in an aqueous ethylenediamine (EDA) solution, optimising the plasma pressure and exposure time.

The braided structures were composed of poly(ethylene terephthalate) (PET) and poly(lactide) (PLA) fibres. Following the functionalisation treatments, a physicochemical characterisation was performed to determine, both quantitatively and qualitatively, the effectiveness of the grafting of primary amine groups on the surface. It was further observed that while the EDA grafting yielded more primary amino groups, the NH_3 plasma treatment conferred more nitrogen-containing groups.

Then, tensile tests were performed to determine if the treatments had an impact on the mechanical performance of the structures. The treated PLA fibres were the most affected, while the treated PET braids remained comparable to the untreated braided structures.

Finally, an *in vitro* biological assay was performed on the samples with the best plasma conditions ($7.5*10^{-2}$ mbar for 12 minutes), and it was determined that while both treatments had improved cell adhesion and proliferation, the NH_3 plasma treatment had better results. This finding qualifies this approach for industrial application, as it is a one-step, sustainable, and easily upscale process.

Keywords: Braided structures, PET fibres, PLA fibres, plasma, cell adhesion and proliferation, tendon and ligament repair

Resumo

Lesões nos tendões e ligamentos são muito frequentes e tendem a impactar a qualidade de vida da população mundial, levando mesmo a alguns profissionais cuja carreira depende diretamente da sua performance física, a uma inesperada e indesejada mudança de profissão. O objetivo primário deste trabalho foi comparar diferentes métodos de funcionalização de estruturas entrançadas de matriz polimérica para a reparação de tendões e ligamentos, para promover a adesão e proliferação celular sem comprometer o comportamento mecânico do dispositivo médico, aumentando o seu sucesso a longo prazo. Os métodos de funcionalização estudados foram baseados num tratamento com plasma de NH_3 assim como plasma de O_2 seguido de imersão numa solução aquosa de etilenodiamina (EDA), otimisando a pressão exercida pelo plasma e o tempo de exposição ao mesmo.

As estruturas fibrosas foram compostas por fibras de poli(etileno tereftalato) (PET) e poli(ácido láctico) (PLA). Após funcionalização, foi realizada a caracterização fisicoquímica das estruturas de modo a determinar, quantitativamente e qualitativamente, a eficiência dos tratamentos aplicados relativamente à presença de grupos amina na superfície dos materiais. Observou-se ainda que as amostras tratadas com plasma de NH_3 apresentaram maior teor de azoto. No entanto, as estruturas modificadas com EDA revelaram maior quantidade de aminas primárias.

Foram também realizados ensaios de tração para averiguar se os tratamentos aplicados teriam impacto no comportamento mecânico das estruturas. As fibras de PLA foram as mais afetadas após tratamento, enquanto que as fibras de PET tratadas mantiveram propriedades mecânicas comparáveis às fibras sem tratamento.

Na fase final da dissertação foi realizado um ensaio biológico *in vitro* nas amostras tratadas com as melhores condições de plasma ($7,5*10^{-2}$ mbar com 12 minutos) e foi observado que ambos os tratamentos aplicados promoveram a adesão e proliferação celular, mas o tratamento com plasma de NH_3 apresentou melhores resultados. Este resultado revela a potencialidade industrial desta abordagem, por ser simples, sustentável e facilmente escalável.

Palavras-chave: Estruturas fibrosas, fibras de PET, fibras de PLA, plasma, adesão e proliferação celular, reparação de tendões e ligamentos

Agradecimentos

Em primeiro lugar gostaria de agradecer à minha orientadora, professora Ascensão Lopes pela exímia disponibilidade para ajudar e por todo o conhecimento que me transmitiu, não só ao longo do desenvolvimento deste trabalho, mas ao longo de todo o meu percurso académico superior, desde o primeiro ano de licenciatura. Quero também agradecer ao professor Raúl Fangueiro pela sua disponibilidade e ajuda.

Quero deixar um agradecimento à Tânia por todo o apoio, pelo conhecimento, e pela amizade, e quero também agradecer ao Miguel por todo conhecimento que me transmitiu e pela amizade.

Aos meus amigos de infância, aos que vêm desde a escola, aos meus colegas de curso, e aos que vieram da partilhada paixão pelas artes, um muito obrigado por todo o apoio e pela partilha de momentos que levarei para toda a vida.

À minha família, um enorme obrigado por todo o incansável apoio, pelas oportunidades, pelos conselhos, pelos bons momentos, e por serem a melhor família que poderia desejar ter.

Contents

Abstract i

Resumo ii

Agradecimentos iii

Figure Index vi

Tables Index viii

Abbreviations and Acronyms ix

1. Introduction 1

1.1. Context and objective 1

1.2. Document outline 2

2. State of the art 3

2.1. Tendons and ligaments 3

2.1.1. Anatomy and function 3

2.1.2. Mechanical behaviour 5

2.1.3. Common injuries 7

2.1.4. Healing process 8

2.2. Current treatment approaches for tendon and ligament injuries 10

2.3. Material selection, textile technology and surface functionalisation 15

2.3.1. Material selection 15

2.3.2. Textile technology and braided structures 17

2.3.3. Surface functionalisation 20

3. Materials and methods 21

3.1. Materials 21

3.2. Production of the braided structures 21

3.3. Surface functionalisation 22

3.4. Mechanical behaviour 24

3.5. Physicochemical characterisation 24
3.6. *In vitro* biological characterisation 26
3.6.1. Resazurin assay 27
3.6.2. Optical microscopy 28
3.6.3. SEM analysis 28
3.7. Statistical analysis 28
4. Results and Discussion 29
4.1. Physicochemical characterisation 29
4.2. Mechanical behaviour 42
4.3. *In vitro* biological characterisation 45
5. Main conclusions and future work 49
References 51

Figure Index

Figure 1: Hierarchical structure of a tendon [10]. 4
Figure 2: Representation of a tendon and enthesis [12]..... 5
Figure 3: a) Representative stress-strain curve of a tendon [15]; b) Representative stress-strain curve of ligaments [15]. 6
Figure 4: Achilles tendon (AT) vs Anterior cruciate ligament (ACL) [17, 18]. 7
Figure 5: Mechanical behaviour of a tendon during the healing process [6]. 8
Figure 6: TissueMend, by Stryker Orthopaedics [21]. 11
Figure 7: Leeds Kuff-Patch [23]. 14
Figure 8: Lars Ligament [24].....14
Figure 9: Yield strength and biodegradability comparison of polymers. 17
Figure 10: Core-shell structure of the medical device [26].....18
Figure 11: Comparison of the mechanical behaviour of braids with varying draw-off speed and yarn number [27].....19
Figure 12: Comparison of the mechanical behaviour between core-shell structure and a braid with 16 yarns [26] 19
Figure 13: Vertical braiding machine system used for braid production (Trenz Export Sa, Spain).....21
Figure 14: Emitech K1050X plasma system used for surface treatment of the braids. 22
Figure 15: Orange II dyed samples, air drying. 25
Figure 16: Braid samples immersed in basic solution, incubating at room temperature at 150 rpm. 25
Figure 17: Vertical wicking test.....26
Figure 18: Braid samples for *in vitro* biological characterisation. 27
Figure 19: Evaluation of amino groups grafting in PET braids by the Orange II method, with varying work pressures. 29
Figure 20: Evaluation of amino groups grafting in PET braids by the Orange II method with varying times of exposure to plasma.....30
Figure 21: Evaluation of functionalisation stability of PET and PLA braids over 4 weeks. 32

Figure 22: Qualitative evaluation of the amino groups' distribution on PET and PLA braids after different treatments. 33
Figure 23: Wicking test of PET and PLA braids, for both NH_3 plasma-treated braids and O_2 plasma-treated braids with immersion in EDA. 34
Figure 24: SEM images of PET braids, with different treatment conditions. 35
Figure 25: SEM images of PLA braids, with different treatment conditions. 36
Figure 26: EDS scan of treated PET and PLA braids. 37
Figure 27: Molecular structure of polu(ethylene terephthalate) [37]. 38
Figure 28: XPS overview and detailed spectra of untreated and treated PET braid39
Figure 29: Molecular structure of poly(lactide) [42]. 40
Figure 30: XPS overview and detailed spectra of untreated and treated PLA braids. 42
Figure 31: Results of the mechanical tests of treated and untreated PET and PLA braids. 43
Figure 32: A) Metabolic activity of fibroblast cells on PET braids, measured up to 21 days by resazurin assay. *$p<0.05$, significant differences from PET, for each time-point. #$p<0.05$, significant differences of EDA from NH_3, for each time-point; B) Growth rate comparing Day 1 to Day 15; C) Microscopic images of fibroblast cells on PET braids, after cells colouring by MTT assay. 46
Figure 33: SEM images of cell adhesion in PET braids treated with NH3 plasma and O2 plasma followed by immersion in EDA, day 15 of the experiment.....47

Tables Index

Table 1: Examples of biological extracellular-matrix products for tendon/ligament repair [5]. 12
Table 2: Examples of synthetic products for tendon/ligament repair [5].....13
Table 3: Plasma treatment parameters: Reactive gas, plasma pressure and exposure time during functionalisation of PET braided structures.....23
Table 4: Plasma treatment parameters: Reactive gas, fixed plasma pressure and exposure time during functionalisation of PET braided structures. 23
Table 5: Plasma treatment parameters: Reactive gas, fixed plasma pressure and fixed exposure time during functionalisation of PET and PLA braided structures...24
Table 6: Chemical bonds and binding energy (eV) of PET samples. Bellow each binding energy is atomic concentration (%).....40
Table 7: Chemical bonds and binding energy (eV) of PLA samples. Bellow each binding energy is atomic concentration (%).....41

Abbreviations and Acronyms

ACL	Anterior cruciate ligament
AT	Achilles tendon
ECM	Extracelular matrix
EDA	Ethylenediamine
EDS	Energy dispersive spectroscopy
FBS	Fetal Bovine Serum
FDA	Food and Drug Administration
MEM	Minimum Essential Medium
MTT	(3-(4,5-Dimethylthiazol-2-yl)-2,5-diphenyltetrazolium bromide)
PBS	Phosphate buffered saline
PCL	Poly(caprolactone)
PET	Poly(ethylene terephthalate)
PGA	Poly(glycolide)
PLA	Poly(lactide)
PLGA	Poly(lactic-glycolic acid)
PLLA	Poly(L-lactide)
PP	Poly(propylene)
RFUs	Relative fluorescence units
SEM	Scanning electron microscopy
UK	United Kingdom
USA	United States of America
UV	Ultra Violet
WNBA	Women's National Basketball Association

XPS	X-ray Photoelectron Spectroscopy

1. Introduction

1.1. Context and objective

Professional athletes and performing artists spend most of their lives practising repetitive and often quite straining movements in order to achieve performative perfection. More often than not, this continuous effort results in very debilitating injuries that may lead to early retirement or loss of physical ability. Up to 50% of patients retire from their sport as a consequence of their injury. Around 75% of professional orchestral musicians may develop a musculoskeletal disorder from playing their respective instruments, and about 1.7 to 6.7 injuries may occur per professional dancer every year [1-3]. Old age may also be a decisive factor, as the prevalence of tendinopathies widens with age [4].

Most of these injuries are due to prolonged overuse of tendons and ligaments. In more severe cases, acute trauma may be the cause, but often the most commonly injured tissues are the ones that are more frequently exposed to repeated stress and strain [5].

These tissues are connective tissues whose function is to allow body movement by transmitting tensile forces from bone to bone or bone to muscle. They are also essential to skeletal and joint stability, and may also absorb excessive external force, thus preventing further muscle damage [6].

The natural healing process, however, is largely inefficient. Apart from being exceedingly slow, it also results in a loss of mechanical performance, which, undoubtedly, may affect the patient's lifestyle and quality of life severely, especially if the patient's line of work depends directly on their physical capabilities. This lack of functionality by the end of recovery is due to the formation of scar-like tissue during the earlier stages, which is never entirely replaced [1, 5, 7].

In order to improve the healing process, a variety of medical devices have been emerging. These include various types of scaffolds: biological scaffolds, which are made of human or animal tissues; natural scaffolds, which include silk and collagen, for example; and finally, synthetic scaffolds, which are the main focus of this work.

These synthetic scaffolds are made of polymers, such as poly(ethylene terephthalate) (PET) and poly(lactide) (PLA), and offer much more controllable and reproducible properties, compared to the previously discussed types. Nonetheless, the challenge lies in the development of a structure that properly supports and allows the healing of the native tissue. [5, 6].

Although synthetic scaffolds are advantageous mechanically, some polymeric surfaces, such as PET, lack surface energy and display poor adhesive properties. This work will explore different approaches to overcome these limitations, which is a key area of the research within the group where the work was developed and is linked to the doctoral thesis of Tânia Peixoto, dedicated to the development of complex hybrid structures for tendon and ligament repair.

1.2. Document outline

The present document is divided into 5 chapters. Chapter 1 describes the context behind the development of this work and its objective. In chapter 2, the state of the art is presented, addressing the anatomy and function of tendons and ligaments, their mechanical behaviour, common injuries and the natural healing process and current approaches for tendon and ligament repair. Then, a brief explanation of the material selection, textile technology and surface functionalisation to apply is presented. Chapter 3 describes the materials and methods used throughout the development of this work, such as the production of the braids and their functionalisation, as well as the characterisation methods used after the application of the treatments. In chapter 4 the results are presented and discussed, including physicochemical and mechanical tests, as well as a biological *in vitro* assay. Finally, the conclusions of this work are presented in chapter 5, followed by future work to be developed.

2. State of the art

2.1. Tendons and ligaments

Achilles tendon injuries can be very desolating, especially for professional athletes, whose career is directly correlated to peak physical health. An example of this is professional basketball players. Studies evaluating the return-to-play rate and performance of players after their return have shown that after an Achilles tendon rupture, even after recovery, 23.5% of players failed to return to the WNBA, while 41.2% failed to play for more than one season [8, 9].

As these injuries are commonplace and quite detrimental to the quality of life of many, several products have come to light in order to aid the recovery of these tissues.

Tendons and ligaments are mainly constituted of fibroblastic cells and an extracellular matrix (ECM), primarily constructed with type I collagen fibres in a highly organised hierarchical structure. Tendons transmit forces from muscle to bone, and ligaments from bone to bone. These connective tissues are essential for locomotion and joint stability [7].

These tissues exist in a wide variety of shapes and sizes, and their respective properties may vary along with the condition and age of the patient [5, 7].

2.1.1. Anatomy and function

Tendons and ligaments display a highly organised hierarchical structure of increasing complexity [6, 7].

These tissues are primarily composed of type I collagen, whose structural unit is termed tropocollagen. Tropocollagen assembles into fibrils in order to form a fibre. These fibres are then assembled in parallel and form a bundle that is involved by the endotenon. These bundles are then further assembled and involved by another

connective tissue, termed the epitenon, and hence the tendon is conceived [6, 7]. This highly organised hierarchical structure of a tendon is illustrated in Figure 1.

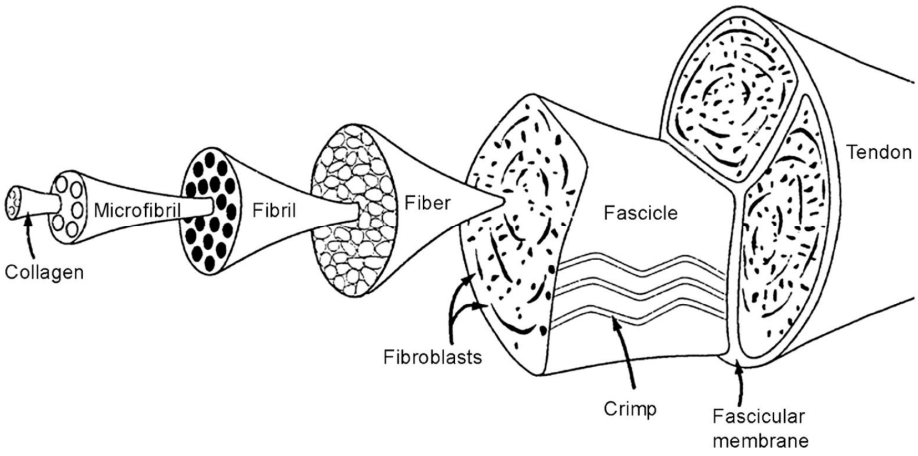


***Figure 1**: Hierarchical structure of a tendon [10].*

The extracellular matrix's components are synthesised by the fibroblasts present in the tissue's constitution, namely tenoblasts (immature cells) and tenocytes (matured tenoblasts). The tendon also includes in its constitution 1 to 2% of elastin that is embedded in a substance made up primarily of water, as well as glycoproteins and proteoglycans, both in residual quantities [6, 7].

In order for tendons and ligaments to connect to bone and muscle, there are specialised areas of tissue at the extremities (Figure 2). These specialised areas are known as fibrous and fibrocartilaginous enthesis, and these constitute the attachments of tendons to bone. In a fibrous enthesis, the tissue attaches directly to the bone. In contrast, in a fibrocartilaginous enthesis, there are transitional zones between the soft tissue and the bone, composed of uncalcified fibrocartilage, calcified fibrocartilage, and finally, bone. Furthermore, the enthesis also reduces peak stress by dissipating it at the junction between the soft tissue and the bone. In a myotendinous junction, which connects tendons to muscle, the transferring of tension across the tendon-muscle interface is permitted due to recesses formed by myocytes, into which the collagen fibrils are inserted [7, 11].

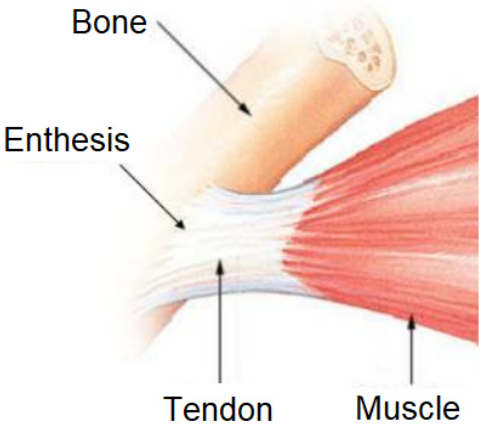


***Figure 2**: Representation of a tendon and enthesis [12].*

Generally, ligaments are tough connective tissues that connect bones, both directly and indirectly, and stabilise kinematic articulations. Direct insertion occurs in the following sequence: ligament, fibrocartilage, mineralised fibrocartilage, and bone. In indirect insertion, on the other hand, the superficial fibres are attached to the periosteum, and the deep fibres are connected to the bone [13].

Ligaments display a hierarchically organised structure, similarly to tendons, and are composed of mainly type I collagen fibres and small amounts of elastin, although proportionally more than tendons [7].

2.1.2. Mechanical behaviour

Both tendons and ligaments display a viscoelastic behaviour when submitted to stress. As an example, the typical stress-strain curves of tendons and ligaments are shown in figure 3 [14].

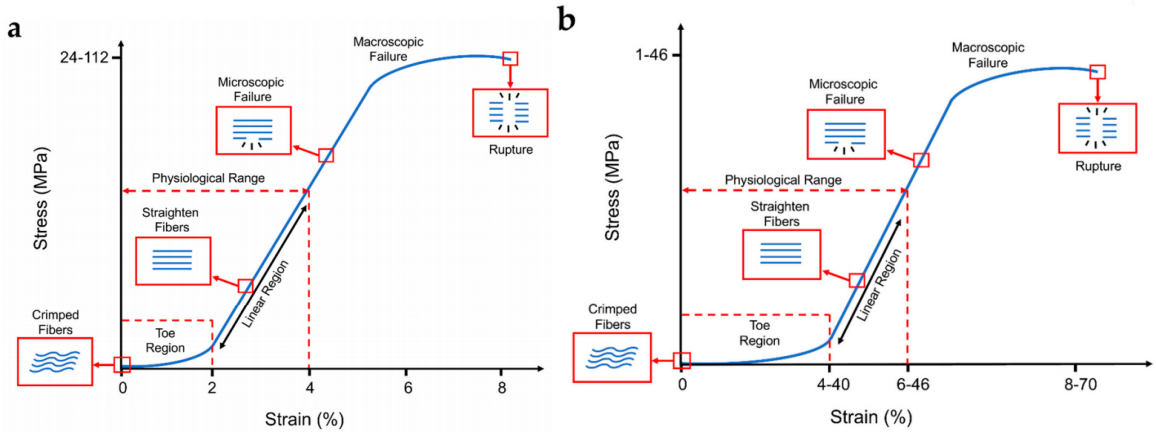


***Figure 3**: a) Representative stress-strain curve of a tendon [15]; b) Representative stress-strain curve of ligaments [15].*

The mechanical behaviour of these tissues is divided into three main stages: the first region, termed the 'toe' region, refers to the initial application of load. In this phase, the tendon is at rest, presenting a wavy configuration that is lost when stretched, gaining a linear arrangement. The collagen fibres begin to deform in the second region, showing a linear response to the increasing strain. Some microscopic tearing may occur. In the third region, the intermolecular crosslinks begin to fail, and the tissue may rupture [14, 16].

While the stress-strain curve of tendons and ligaments may appear similar, it is essential to note the difference in the range of stress and strain, represented in figure 3.

The mechanical properties of tendons and ligaments also diminish with age, as shown in figure 4 [17, 18].

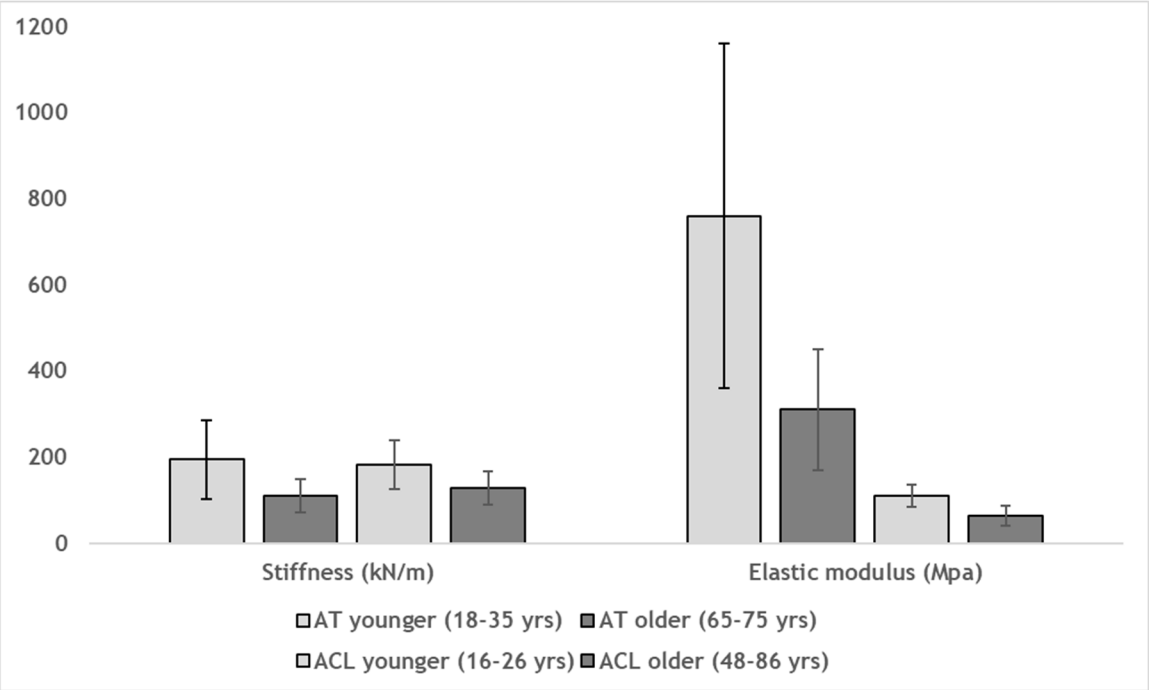


***Figure 4**: Achilles tendon (AT) vs Anterior cruciate ligament (ACL) [17, 18].*

2.1.3. Common injuries

Tendon and ligament injuries usually stem from degenerative disorders, chronic overuse (damage accumulation), and acute trauma (excessive loading) [6].

Common tendon pathologies occur due to overload and overuse, causing lesions or even rupture. Tendinitis is caused by acute overload, causing micro-tears in the tissue. It is characterised as an inflammatory degeneration of the tissue. Tendinosis is caused by continued overuse, causing the degradation of collagen fibres. It is described as non-inflammatory tissue degeneration. The complete rupture of a tendon can also occur when excessive load is applied [6].

Connective tissues under the highest stress and repeated strain, as well as the less vascularised, are the most frequently damaged. One example is the Achilles tendon, which is the most commonly ruptured tendon in the human body, usually during the practice of sports. The presence of pathology and injury on this tendon is also more prevalent as age increases. Moreover, other injuries may occur during the practice of performing arts, such as dancing or playing a musical instrument, as these require repetitive movements over long periods of time [1, 4-6].

2.1.4. Healing process

Tendons and ligaments heal in a prolonged and inefficient manner. These connective tissues do not restore their properties entirely due to the fact that they do not respond to injury with a tissue regeneration process, but rather heal through a wound repair process that includes the formation of fibrous, scar-like tissue in the earlier stages, which is not entirely replaced by the end of the healing process. This results in inferior mechanical performance, compared to healthy tissue, which increases the chance of recurring rupture [6, 19].

As shown in Figure 5, the healing process can be divided into three stages: the inflammation stage, the proliferation stage, and the remodelling stage. These phases may overlap, and their duration and timing may change in accordance with the type of the injury, how severe it is, the condition of the patient, the tissue location, and the applied treatment [6, 19, 20].

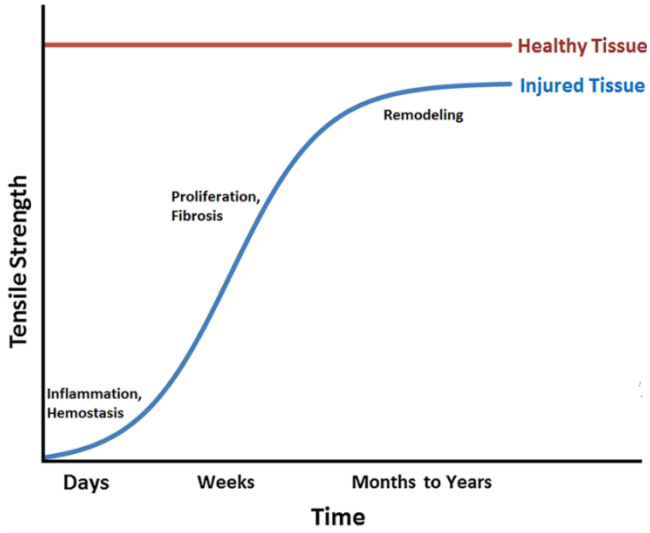


***Figure 5**: Mechanical behaviour of a tendon during the healing process [6].*

The inflammatory phase is the shortest, lasting days. It begins immediately after the occurrence of acute injury and starts with increasing the vascular permeability and the recruitment of inflammatory cells into the injury site. These include platelets, macrophages, monocytes, and neutrophils, which release vasoactive and

chemoactive factors, culminating in the recruitment of blood vessels, fibroblasts, and intrinsic tenocytes, consequently contributing to ECM deposition and remodelling [10, 20].

The proliferation phase, which may last weeks, consists of the multiplication of fibroblasts at the injury site and the synthesis of type III collagen, which is responsible for the repair of partial tissue continuity, as well as providing a scaffold for the migration of recruited cells into the wound area. Other ECM components are also synthesised [10, 20].

The remodelling phase, which may last months, displays a remarkable decrease in cellularity and vascularity in comparison to the previous phases. The synthesised type III collagen gradually remodels into type I collagen; collagen is crosslinked and aligned with the direction of muscle force, which increases tissue stiffness. The fibrovascular scar that forms during the earlier stages of the healing process is never entirely replaced, resulting in a loss of mechanical performance [5, 6, 10, 20].

By the end of the process, the tissue may only restore a portion of its previous mechanical properties. Thus, the improvement of the efficiency of this healing process is vital to repair the functionality of the injured tissue fully. In order to boost this healing process, human intervention is imperative.

2.2. Current treatment approaches for tendon and ligament injuries

When the injury is of a low degree, conservative management may be used as a first approach to relieve the pain. This includes rest, mechanical conditioning, injection of corticosteroids, orthotics, ultrasound, laser, or shockwave treatment [6].

However, due to the aforementioned limitations of the self-healing process, such as the formation of scar tissue and the loss of critical mechanical properties, surgical intervention is often necessary [6, 19].

Surgical intervention is used to suture the ends of the injured tissue together, or to fix the tendon to the bone. However, this process may fail as a result of the limitations of the self-healing mechanism of the involved tissues, which can be improved by injecting growth factors and therapeutic cells into the damaged tissue [6].

Biological scaffolds are protein-based ECM, consisting of human or animal tissues such as the dermis, small intestine, or pericardium. These tissues are processed in order to remove non-collagen components, so that one may minimise the risk of rejection by the patient, but nonetheless maintain its natural collagen fibrous structure, providing a faster and better host-cell integration. Despite that, remaining trace chemicals may be toxic to the host cells, and these scaffolds may have biocompatibility variations, undefined degradation rates, and too low mechanical properties [5, 6].

Natural scaffolds, on the other hand, present much higher bio-functionality, biocompatibility and biodegradation when compared to synthetic scaffolds. However, they display a variety of limitations as well. These include limited processability, wide variability from batch to batch and overall lower mechanical properties [6].

A few of these devices are presented in table 1. Most of these devices are in the form of patches, aiming to aid in the restoration of the normal function of the tissue

by providing mechanical augmentation; that is, they may provide both protection after small ruptures, as well as aid in its mechanical function, not allowing excessive loads to be applied, thus offering the support for the repair process to occur [5].



***Figure 6**: TissueMend, by Stryker Orthopaedics [21].*

One example is TissueMend by Stryker Orthopaedics, illustrated in figure 6, which is a collagen membrane aiming to reinforce the soft tissues repaired by sutures in tendon repair surgery [21].

***Table 1**: Examples of biological extracellular-matrix products for tendon/ligament repair [5].*

Category	*Product name*	*ECM type*	*ECM source*	*Marketed by*
Augmentation device	Restore	SIS	Porcine	Depuy Orthopaedics (USA)
	CuffPatch	SIS (crosslinked)	Porcine	Arthrotek (USA)
	GraftJacket	Dermis	Human	Wright Medical (USA)
	ArthroFlex	Dermis	Human	Arthrex (USA)
	Conexa	Dermis	Porcine	Tornier (USA)
	TissueMend	Dermis (fetal)	Bovine	Stryker Orthopaedics (USA)
	Zimmer Collagen Repair	Dermis (crosslinked)	Porcine	Zimmer (USA)
	Bio-Blanket	Dermis (crosslinked	Bovine	Kensey Nash (USA)
	OrthADAPT Bioimplant	Pericardium (crosslinked)	Equine	Pegasus Biologics (USA)

In order to counter the inferior mechanical properties of both natural and biological scaffolds, plentiful synthetic scaffolds have come to light. These are mainly derived from polymers such as poly(glycolide) (PGA), poly(lactide) (PLA), poly(caprolactone) (PCL), poly(L-lactide) (PLLA) and poly(lactic-glycolic acid) (PLGA). Synthetic scaffolds, when compared to natural scaffolds, achieve much more controllable and reproducible mechanical, chemical and degradation properties, as well as their shape and size, given the improved batch to batch uniformity. These, however, present a few drawbacks; for instance, the absence of functional chemical groups involved in cell adhesion, as well as the potential release of acidic by-products into the bloodstream as a consequence of degradation, which may cause adverse reactions [5, 6].

Presented in Table 2 are a variety of examples of synthetic medical devices for tendon and ligament repair. Both the Leeds-Keio (Neoligaments, UK) and the Lars Ligament (Lars, France) are mainly made of poly(ethylene terephthalate) (PET). The first is a woven porous tube attached to woven tapes, while the second is manufactured in a broad range of sizes and shapes, in order to provide the necessary functionality. The Kennedy ligament, on the other hand, is made of poly(propylene) (PP). It is produced in a diamond-braided structure [5, 22].

***Table 2**: Examples of synthetic products for tendon/ligament repair [5].*

Category	*Product name*	*Material*	*Marketed by*
Augmentation device	SportMesh	Poly(urethane urea)	Biomimet Sports Medicine (USA)
	X-Repair	Poly-L-lactide	Synthasome (USA)
	Biomerix Patch	Polycarbonate poly(urethaneurea)	Biomerix (USA)
	Gore-Tex	Poly(tetrafluoroethylene)	WL Gore and Associates (USA)
	Kennedy Ligament	Polypropylene	DAW Industries, 3M (USA)
	Leeds-Kuff Patch	Polyester	Neoligaments (UK)
	Rota-Lok	Polyester	Neoligaments (UK)
	AchilloCordPLUS	Poly(ethylene terephthalate)	Neoligaments (UK)
Prosthetic device	OrthoCoupler	Poly(ethylene terephthalate)	Surgical Energetics (USA)
	Lars Ligament	Poly(ethylene terephthalate)	Lars (France)
	Leeds-Keio	Poly(ethylene terephthalate)	Neoligaments (UK)

Products such as the Leeds-Kuff Patch, shown in figure 7, have been designed in order to promote tissue regeneration, and to be permanently implanted. It is constructed from knitted polyester [22, 23].

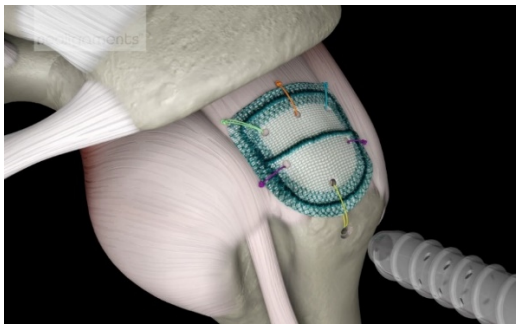


***Figure 7**: Leeds Kuff-Patch [23].*

Products such as Lars Ligament, shown in figure 8, on the other hand, are indeed intended to reinforce the damaged tissue mechanically. However, these are built of non-biodegradable materials such as PET, given their adequate mechanical properties; therefore, they are permanent implants [22, 24].



***Figure 8**: Lars Ligament [24].*

While these synthetic devices may offer the required functionality to replace the injured tissue in the earlier stages, they fail over long periods of time, as they cannot wholly replace the mechanical response of the native tissue, which may lead to permanent deformation as a consequence of repeated strain, and may fail in the long term, deriving from problems such as fatigue [22].

2.3. Material selection, textile technology and surface functionalisation

2.3.1. Material selection

Ideally, a scaffold for tendon and ligament repair should possess a porous, biocompatible structure, in order to further support cell adhesion, new tissue formation, growth and integration. This scaffold should also sufficiently replace the mechanical attributes of the original tissue, as to temporarily maintain the mechanical function of the native tissue in order to allow the healing process to occur appropriately [5].

Material selection is of pivotal importance. The chosen material should not cause inflammation or any other adverse reactions that could hinder the healing process or cause the body to reject it. Moreover, it may allow the final fibrous structure to mimic the viscoelastic behaviour of the original tissues. This may also be accomplished while degradation to allow tissue growth and integration occurs [5].

Prominently used biodegradable materials in scaffold production fall into two categories: synthetic or naturally derived. Natural scaffolds, such as silk or collagen, for example, present higher bio-functionality, biocompatibility and biodegradation. These are biologically recognised by the body and are able to provide a better environment to support tissue healing. However, their limited processability and unpredictability due to high variability from batch to batch are substantial disadvantages [5, 6].

As for synthetic polymers, their properties are much more straightforward to control and reproduce. This includes mechanical and chemical properties, as well as degradation properties. Poly(glycolide) (PGA), poly(lactide) (PLA), poly(lactic-glycolic acid) (PLGA), and poly(caprolactone) (PCL) are all decidedly inviting polymers, with biodegradable properties, utilised in medical applications. These materials are also approved by the Food and Drug Administration (FDA) for clinical use and are considered biocompatible. Furthermore, these materials normally degrade into non-toxic components, which are then either excreted by the human body, or metabolised by it [5, 6].

Although biocompatible and biodegradable polymers exhibit numerous advantages, many challenges still remain to be overcome. These materials are usually inferior when considering their mechanical performance, compared to that of native tissues. Moreover, the decreased mechanical compatibility between the native tissue and the implemented medical device may interfere with the self-healing process, hindering its repair and growth, and in some cases leading to failure. Furthermore, the needed balance between gradual degradability and native tissue healing and growth is still challenging to accomplish [5].

Another challenge lies in the development of a structure that efficiently supports the mechanical function of the tissue during the repair period [6].

In order to properly develop an implantable device, many vital aspects must be taken into consideration. Implants for tendon and ligament repair are usually strong and flexible materials. However, the mechanical efficiency of the material is not enough for a medical device, as there are many other safety aspects that are key to the proper development of these products. Toxicity and release of toxic substances are critical to the safety of the patient. These may cause an adverse body reaction to the device, and the release of harmful substances may be fatal. The porosity of the material is also to be taken into account, as it is essential to proper native tissue growth and integration. Lastly, biodegradability is fundamental for this particular application. If the material is biodegradable, then, ideally, the native tissue would grow and gradually integrate and replace the medical device [25].

While previously built braids were composed of both poly(propylene) (PP) and poly(ethylene terephthalate) (PET), it is essential to note that neither of these is biodegradable [26]. Therefore, poly(lactide) (PLA) may constitute an efficient alternative, as it is derived from natural materials, starch and cellulose, and is entirely biodegradable [25].

Considering the final application of the medical device, which is a hybrid structure composed of PET and PLA fibres, both these materials should have somewhat similar elastic regions, so as to avoid any irreversible plastic deformation. Therefore, the elastic limit of each material that composes the hybrid structure should be similar. In figure 9 is presented a schematic of biocompatible polymers, organised by tensile strength (MPa) and biodegradability, using the GRANTA EduPack

software. This schematic was obtained by limiting the materials shown to biomedical polymers of medical grade used in grafts and patches.

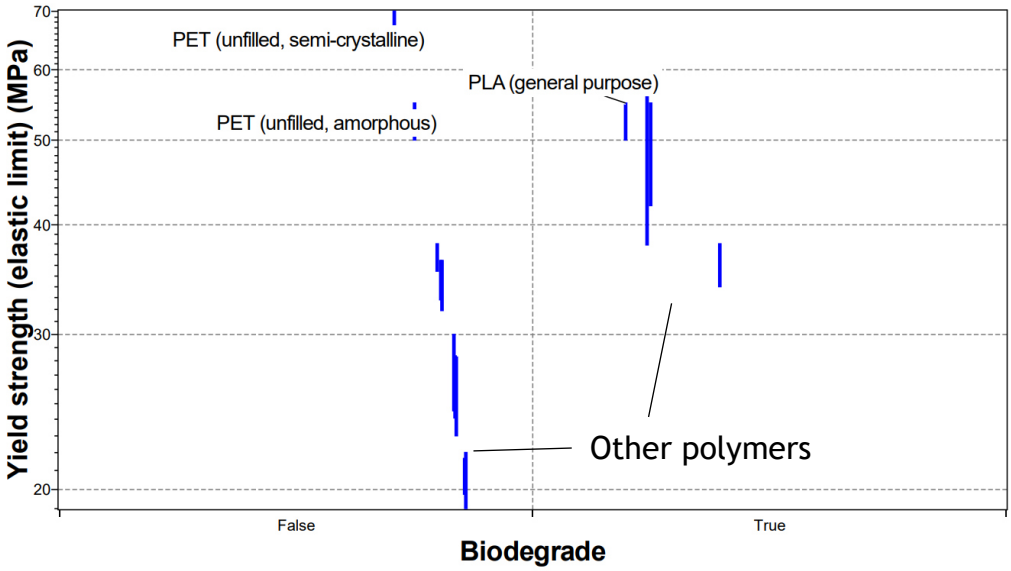


***Figure 9**: Yield strength and biodegradability comparison of biocompatible polymers.*

Accordingly, a combination of PLA and PET's properties may be adequate, when combined in a hybrid structure, based on a core/shell system. Whereas PLA is biodegradable, PET is not; however, given its superior mechanical performance, it would serve as a reinforcement in order to achieve mechanical prowess. Thus, PET yarns would serve the primary mechanical function, while PLA would provide porosity in the structure, after degrading, allowing for tissue integration and degradation.

2.3.2. Textile technology and braided structures

Medical devices with a hierarchical fibrous structure (rope-like structure) have previously been conceived through textile techniques by our research group. These structures attempt to replace the mechanical function of a tendon to allow its healing process to occur. These ropes are composed of braids bundled together and enveloped by a shell. These braids, as well as the shell, are composed of yarns of a certain biocompatible material, such as PET, PP and PLA, which were braided by the use of a vertical braiding machine. These structures resemble the hierarchical structure of tendons. This resemblance lies in the arrangement of a simple unit into

a more and more complex structure [26]. This results in a core-shell structure, illustrated in figure 10.

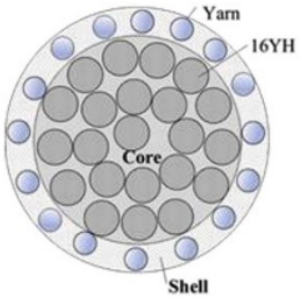


***Figure 10**: Core-shell structure of the medical device [26].*

In the case of a hybrid structure of PET and PLA for tendon and ligament repair, PET would provide its high mechanical performance, whereas PLA would provide porosity after degrading in order to promote and support native tissue integration and growth. This is possible due to its biodegradability, shown in figure 9.

There are a few key variables that need to be kept in mind when producing these braids and ropes, in order to properly reproduce their characteristics in a controlled and efficient manner. These include the type and diameter of the yarn, the draw-off speed, the braiding angle of the sub-components, as well as their diameter and number, and the tension applied on the yarns, as well as on the sub-components, the bonding type and finally, the possible post-production treatments [26].

Previous results by our research group have shown that the stress-strain curve obtained is directly influenced by the braid angle, which is itself directly influenced by the draw-off speed. Further results have shown that the braids produced with lower draw-off speed, and consequently higher braid angle, displayed more strain at failure. Figure 11 shows the behaviour of the mentioned braids [27].

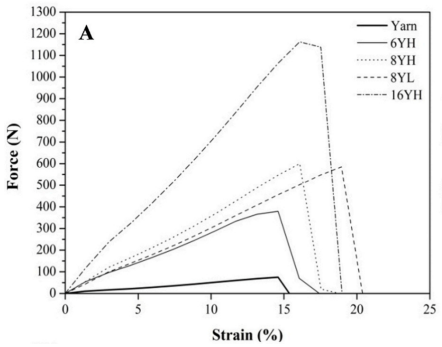


***Figure 11**: Comparison of the mechanical behaviour of braids with varying draw-off speed and yarn number [27].*

The 8YL ropes are composed of eight yarns produced at a lower draw-off speed. Similarly, 8YH is composed of eight yarns produced at a higher draw-off speed. Thus, The conclusion that lower draw-off speed and its consequent higher braid angle results in a higher strain at failure is drawn.

Our research group has determined, in previous works, that the structure with the best mechanical performance is constituted of 22 PET braids with 16 PET yarns each, braided at the highest take-up rate setting, as the core, and 16 yarns braided as a shell, enveloping the core [26]. The mechanical performance of this final structure is illustrated in figure 12, in comparison to the mechanical performance of a single braid that composes the final structure's core.

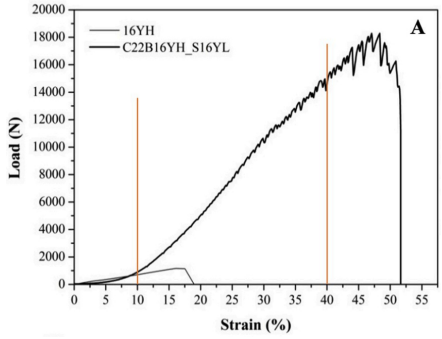


***Figure 12**: Comparison of the mechanical behaviour between core-shell structure and a braid with 16 yarns [26]*

The braiding angle can be considered one of the most crucial parameters in the process of braiding. It is determined by the angle between braided yarns and the

longitudinal direction. The braiding angle can be manipulated during the process in order to create braided structures with different assets: that is, the braiding angle can affect pore size and the mechanical properties of the structure [28].

If the braiding angle increases, the pore size decreases in the fabric, which can tweak cell growth on the braided structure. Moreover, an increase in the braiding angle leads to the yarns moving further away from the longitudinal axis, thus requiring more force to align with the longitudinal direction and increasing the length of the toe region. Similarly, a decreased braid angle produces a stiffer scaffold [28].

The diameter is another essential parameter to keep in mind in braiding. It can be easily changed along with the number of fibres used. Different diameters can be attained to achieve different properties, as well as improve compatibility in specific applications [28].

2.3.3. Surface functionalisation

Although synthetic scaffolds are advantageous mechanically, some polymeric surfaces, such as PET, lack surface energy and display poor adhesive properties. However, techniques such as the activation of the polymer surface by plasma are able to overcome these limitations [29].

Plasma treatments have been used to enhance the culturing of cells and improve the biocompatibility of polymer materials, as well as for cleaning biomedical material surfaces [30].

Previously tested PET structures suffered from low wettability due to low surface energy and the absence of active functional groups, which hindered the cell adhesion process. So, the chemical grafting of amino groups (-NH_2) on the PET surface was employed. This was done by activating the surface with oxygen plasma, and then soaking the structures in a 50% v/v EDA (Ethylenediamine, $C_2H_8N_2$) solution. The anime groups should couple with the PET surface by one amine side, leaving the other available to react with the ECM macromolecules [31].

3. Materials and methods

3.1. Materials

PET multifilament yarn, with 192 filaments and a linear density of 1100 dtex, was purchased from Sarla Europe (Portugal), and PLA multifilament yarn with 108 filaments was bought from Senbis Polymer (Netherlands).

3.2. Production of the braided structures

These braided structures were produced using a vertical braiding machine with 16 carriers (Trenz Export Sa, Spain). The conditions were set so as to maintain a take-up rate of around 3.96 cm/s. All 16 carriers were loaded with only PET yarns, and then only PLA yarns, in order to produce PET braids and PLA braids with 16 yarns. Figure 13 illustrates the system used.

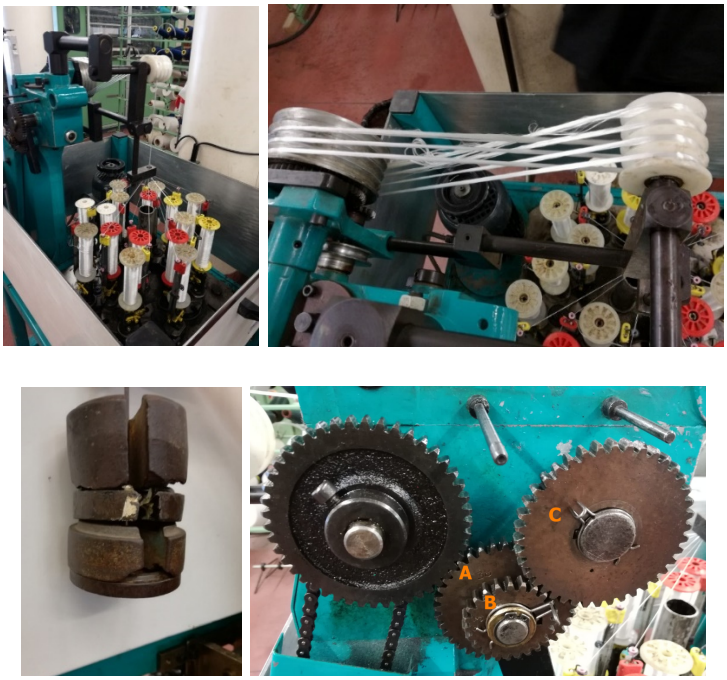


***Figure 13**: Vertical braiding machine system used for braid production (Trenz Export Sa, Spain).*

As seen in figure 13, the gears and weight at the end of the braid were used so as to attain a similar take-up rate to the previous structure developed by the research group.

3.3. Surface functionalisation

The produced braided structures were exposed to different plasma treatments in an Emitech K1050X plasma system (figure 14). The different plasma treatments were performed using O_2 and NH_3 gases with 99.999% and 99.99% purity, respectively. The reactive plasmas were produced with 100W power.

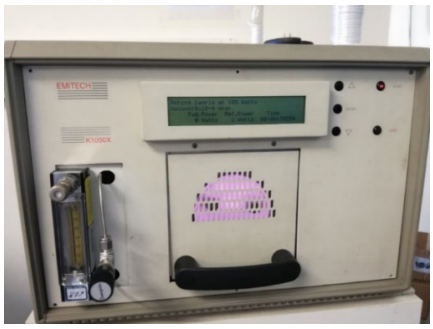


***Figure 14**: Emitech K1050X plasma system used for surface treatment of the braids.*

All plasma treatments were applied on the braided structures, as opposed to the multifilament yarns, since the application of the plasma on the filaments directly could hinder the production of the braids afterwards due to expected changes on the surface.

Firstly, the functionalisation parameters were optimised by studying the effect of the plasma pressure on PET braids. The braids were exposed to 8 and 12 minutes of each plasma (O_2 and NH_3). Immediately after each O_2 plasma treatment, PET samples were immersed in an EDA solution, using water as solvent (50 % v/v), at 50 ºC and 20 minutes. These conditions were based on previous findings obtained by the group [31]. After the immersion, the samples were removed from the solutions and rinsed in distilled water. Table 3 summarises the treatment conditions performed.

***Table 3**: Plasma treatment parameters: Reactive gas, plasma pressure and exposure time during functionalisation of PET braided structures.*

Sample name	Reactive gas	Plasma pressure (mbar)	Exposure time (min)
PET_NH_3_7.5_8	NH_3	7.5×10^{-2}	8
PET_NH_3_7.5_12			12
PET_NH_3_1_8		1.1×10^{-1}	8
PET_NH_3_1_12			12
PET_ EDA_7.5_8	O_2	7.5×10^{-2}	8
PET_ EDA_7.5_12			12
PET_ EDA_1_8		1.1×10^{-1}	8
PET_ EDA_1_12			12

Then, the plasma pressure of 7.5×10^{-2} mbar was maintained, and new exposure times were tested (3 minutes and 20 minutes), summarised in table 4.

***Table 4**: Plasma treatment parameters: Reactive gas, fixed plasma pressure and exposure time during functionalisation of PET braided structures.*

Sample name	Reactive gas	Plasma Pressure (mbar)	Exposure time (min)
PET_NH_3_7.5_3	NH_3	7.5×10^{-2}	3
PET_NH_3_7.5_8			8
PET_NH_3_7.5_12			12
PET_NH_3_7.5_20			20
PET_ EDA_7.5_3	O_2	7.5×10^{-2}	3
PET_ EDA_7.5_8			8
PET_ EDA_7.5_12			12
PET_ EDA_7.5_20			20

Then, the parameters of 12 minutes of exposure time and plasma pressure of $7.5*10^{-2}$ mbar were applied to the PLA braids, summarised in table 5.

***Table 5**: Plasma treatment parameters: Reactive gas, fixed plasma pressure and fixed exposure time during functionalisation of PET and PLA braided structures.*

Sample name	Reactive gas	Plasma Pressure (mbar)	Exposure time (min)
PET_NH_3_7.5_12 PLA_NH_3_7.5_12	NH_3	7.5×10^{-2}	12
PET_ EDA_7.5_12 PLA_ EDA_7.5_12	O_2	7.5×10^{-2}	12

3.4. Mechanical behaviour

In order to determine the effect of the various surface treatment conditions on the mechanical behaviour of the braids, a series of uniaxial tensile tests were executed; namely, three per treatment condition.

Each sample was set at a distance of 235 mm between grips, with a displacement rate of 8.5 mm/s.

The equipment used to perform the tests was a Lloyd instruments LR30K tensile testing machine with a load cell of 2.5 kN.

3.5. Physicochemical characterisation

The detection of amino groups was done quantitatively and qualitatively.

The quantification of primary amino groups was determined by the Orange II dye method. The grafted PET and PLA samples, measuring ~ 5 cm, were immersed in 20 mL of dye acidic solution (14 mg/mL) (pH 3) and incubated for one hour at 40 ºC at 150 rpm. After that, the samples were washed with an acidic solution (pH 3) to remove the non-reacted dye, and left to air-dry overnight (figure 15).



***Figure 15**: Orange II dyed samples, air drying.*

After air-drying, the samples were immersed in 5 mL of a basic solution (pH 12) and incubated for 20 min at room temperature at 150 rpm (figure 16).



***Figure 16**: Braid samples immersed in basic solution, incubating at room temperature at 150 rpm.*

The absorbance of the solution was determined at a wavelength of 485 nm in a UV spectrophotometer (UV-1800 Shimadzu, Japan), using quartz cells with a 10 mm path length.

The qualitative method of detecting the presence of amino groups in PET was by staining the filaments with fuchsin acid at pH 2.7, which gives visual information about the concentration and location of the amino groups throughout the braids [31].

The grafted PET and PLA samples were stained with a 0.5% fuchsin acid in pH 2.7 buffer solution, while maintaining agitation for 90 minutes at room temperature. The braids were then rinsed with the same pH 2.7 buffer solution to remove the non-linked dye.

The surface chemistry was evaluated by X-ray Photoelectron Spectroscopy (XPS) using a Kratos Axis Ultra HAS spectrometer with the VISION software for data acquisition. The analysis was carried out with a monochromatic Al X-ray source, operating at 15 kV (90 W), with a pass energy of 40 eV for regions of interest and 160 eV for the overall surveys.

A vertical wicking test (figure 17) was also performed on each treatment condition. Each braid was cut in samples of 250mm in length, then suspended vertically on a stand. The braid was held on one end by a claw, while the other end was submerged in coloured distilled water. The height at which the water had risen was measured every minute over ten minutes.

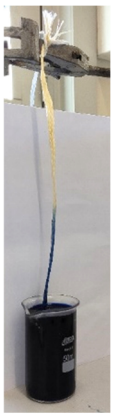


Figure 17: *Vertical wicking test.*

All scanning electron microscopy (SEM) analyses were performed in a FEI Quanta 400FEG microscope (ThermiFisher Scientific), in order to observe possible changes in the surface.

3.6. *In vitro* biological characterisation

Two treatment conditions, namely the NH_3 plasma treated with 12 minutes of exposure and the O_2 plasma treatment with 12 minutes of exposure followed by immersion in an EDA solution, were *in vitro* assessed. The braids were cut into samples of around 2cm in length each, and the edges of each sample were stuck with agar in order for the structure to stay the same throughout the process. These samples are presented in figure 18.



***Figure 18**: Braid samples for in vitro biological characterisation.*

Human dermal fibroblasts (Coriell Institute) were cultured in alpha-Minimal Essential Medium (α-MEM, Gibco) supplemented with 10% (V/V) fetal bovine serum (FBS, Gibco), 100 U/mL penicillin, 100 µg/mL streptomycin, 0.25 µg/mL amphotericin B (all from Gibco). Cells were seeded at two different locations, at $1x10^4$ cells per 2µL per location on each braid, namely untreated PET, NH_3 plasma-treated PET, and O_2 plasma-treated PET with immersion in EDA. The plates were incubated for 1, 3, 6, 9, 12, 15 and 21 days at 37 ºC, in a 5% CO_2 humidified atmosphere.

3.6.1. Resazurin assay

In order to quantitatively determine the metabolic activity of the seeded cells on each sample, a resazurin assay was performed.

At each time point (1, 3, 6, 9, 12, 15 and 21 days), the medium was removed, and the seeded materials were incubated with a medium containing 10% resazurin (0.1 mg/mL, Sigma-Aldrich). The plates were incubated for 3 hours at 37 ºC in a 5% CO_2 humidified atmosphere.

Then, the fluorescence (excitation: 530 nm; emission: 590 nm) was measured in a microplate reader (Synergy HT, Biotek). Results are presented as relative fluorescence units (RFUs).

After each time point, two samples were removed from the batch for the following analysis in section 3.6.2. and 3.6.3.. So, at the first time point (day 1 of the experiment), a total of 16 samples were used. Then, on day 3 of the experiment, a total of 14 samples were used, and so on over the course of the experiment. At the final time point (day 21 of the experiment), a total of 4 samples were used for the resazurin assay.

3.6.2. Optical microscopy

The observation of the cell distribution on the braids was performed on a Zeiss Stemi 508 Stereo Microscope. At each time point, the cells were coloured by the ability of mitochondrial dehydrogenase to reduce the MTT [3-(4,5-dimethylthiazol-2-yl)-2,5,diphenyltetrazolium] to a dark blue formazan product. Briefly, the seeded materials were incubated with a medium containing 10% MTT (0.5 mg/mL, Sigma-Aldrich) for 2 hours at 37 ºC in a 5% CO_2 humidified atmosphere, and then visualised.

3.6.3. SEM analysis

The morphology of the Dermal Fibroblasts seeded on the braids was analysed by SEM using a FEI Quanta 400 FEG ESEM microscope.

All braid samples were washed with PBS and fixed with 1.5% (V/V) glutaraldehyde in sodium cacodylate buffer (pH 7.3) over 15 min. Afterwards, samples were dehydrated using graded ethanol solutions from 50 % (V/V) to 100% (V/V), and critical point dried (CPD 7501, Polaron Range). Finally, samples were sputter-coated (SPI-Module) with a thin gold/palladium film and visualised.

3.7. Statistical analysis

Data is presented as mean value ± SD. Statistical differences between groups of data were tested using t-tests, and were considered significant at a level of $p < 0.05$.

4. Results and Discussion

The experimental work of this dissertation is part of the optimisation of the complex hybrid structures to regenerate tendons and ligaments that have been pursued by the research group where the work was developed. More specifically, this dissertation intended to propose an approach that stimulates cell adhesion to braids, which are the basis for constructing complex hybrid structures.

4.1. Physicochemical characterisation

In order to compare the effect of the NH_3 plasma and O_2 plasma treatment followed by immersion in an EDA solution on the functionalisation of the braids, an analysis was done by the Orange II method, which is used to quantify primary amine groups [32]. This initial analysis was performed in order to determine the effect of the work pressure of each plasma on the amino group grafting on the braids. The results are presented in figure 19.

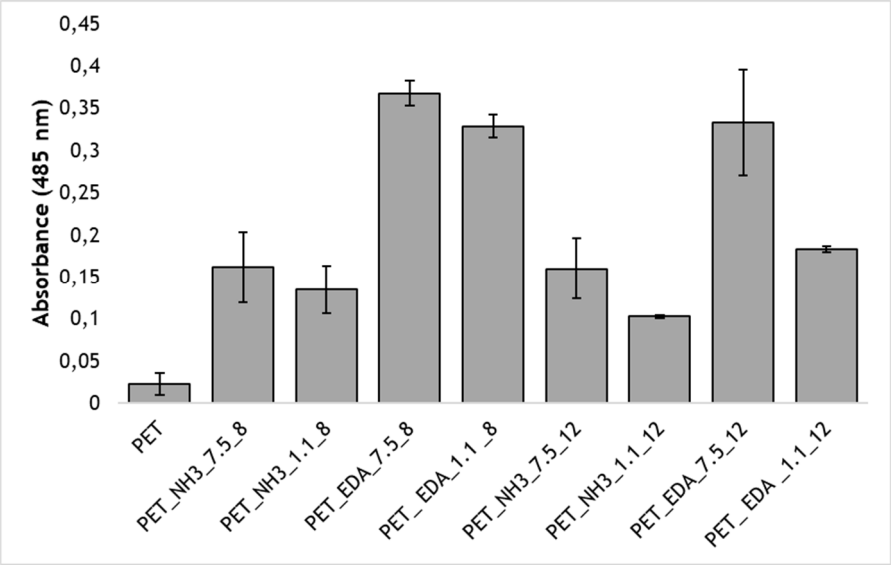


***Figure 19**: Evaluation of amino groups grafting in PET braids by the Orange II method, with varying work pressures.*

The first studied conditions were 8 and 12 minutes of exposure to NH_3 and O_2 plasma, at the work pressures of $7.5*10^{-2}$ mbar and $1.1*10^{-1}$ mbar, being the O_2 plasma-treated braids immersed in an EDA solution for 20 minutes after plasma exposure.

Considering the results presented in figure 19, it was concluded that the increase of the plasma pressure from $7.5*10^{-2}$ mbar to $1.1*10^{-1}$ mbar significantly decreased ($p<0.05$) the absorbance of the samples, which means less amino group grafting.

It is likely that increasing the plasma pressure applied on the braids induced additional roughening on the fibres' surface, due to the effect of thermal heating and etching, which may have led to material degradation [33, 34].

Then, the pressure of $7.5*10^{-2}$ mbar ($p<0.05$), which showed better results, was applied to more plasma treatments with additional exposure to plasma times, including 3 and 20 minutes of exposure, in order to evaluate the impact of the variable of time of exposure to the plasma has on the braid.

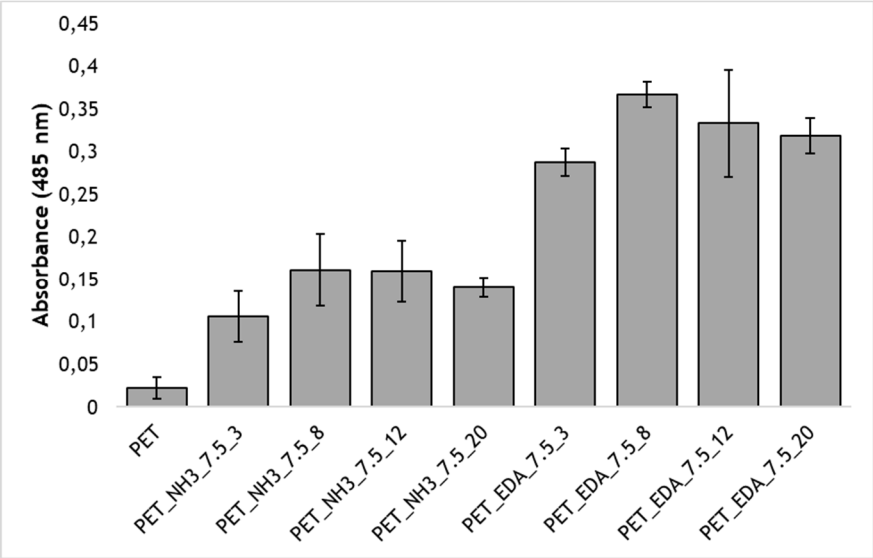


***Figure 20**: Evaluation of amino groups grafting in PET braids by the Orange II method with varying times of exposure to plasma.*

Following these results, presented in figure 20, it was observed that the PET_NH3_7.5_3 braids had significantly lower ($p<0.05$) grafting than the braids

treated with 8 and 12 minutes of exposure. Furthermore, it was determined that the PET_EDA_7.5_3 braids had significantly lower grafting than the braids exposed to 8 minutes of plasma, and that the PET_EDA_7.5_20 braids also had significantly lower grafting compared to the PET_EDA_7.5_8 braid. No other significant differences were found among the various treatment methods. Similarly to the increase in plasma pressure, when using an increased time of exposure to plasma (20 minutes), the etching effect may have overcome the grafting on the surface, while the usage of a lower exposure time may have led to an unsatisfactory grafting of the braids [30, 33, 34].

Since the final medical device is meant to be a hybrid structure consisting of both PET and PLA braids, this same analysis was done on the PLA braids. The treatments and tests were applied on braids of each material in order to evaluate the effectiveness of the grafting and the difference between the materials.

The conditions chosen for the second phase of testing, involving PLA, were 12 minutes of oxygen plasma followed by immersion in a 50% v/v EDA solution, and 12 minutes of ammonia plasma, both with a working pressure of $7.5*10^{-2}$ mbar. These conditions were chosen based on the results presented in figure 19 and 20, namely the fact that this work pressure displayed a better functionalisation, and that the 12 minutes of exposure time was considered to be a balanced choice among the higher exposure times (8, 12 and 20 minutes). An analysis up to the fourth week after treatment was also done in order to evaluate if there was a decay of the functionalisation, which will have an impact on the shelf life of the braids. The results are shown in figure 21.

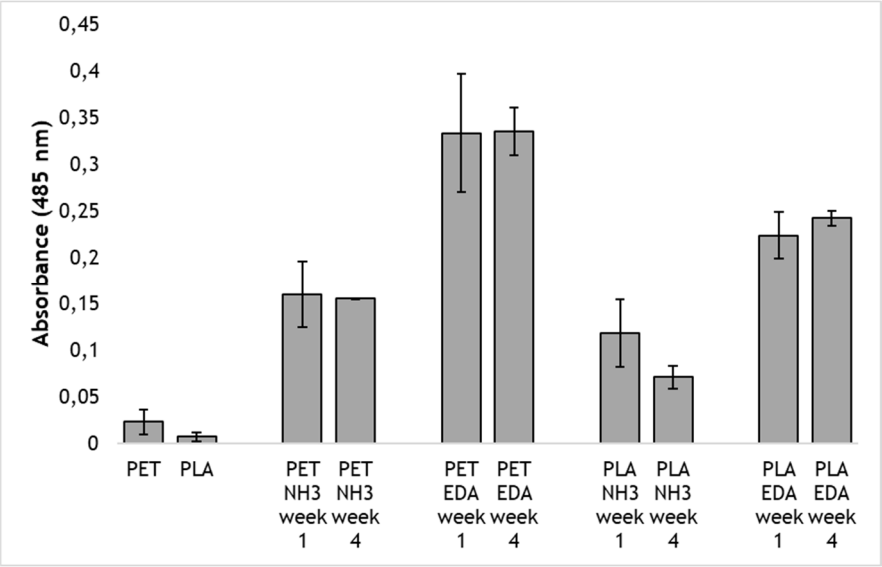


***Figure 21**: Evaluation of functionalisation stability of PET and PLA braids over 4 weeks.*

This final analysis presented in figure 21 served two purposes. Firstly, it was verified that the functionalisation of both materials with either treatment method did not decay over time, as this was tested on the fourth week after treatment, and no significant differences were found ($p<0.05$), which confirmed the stability of the treatment, as the formed surface bonds did not break over time. Furthermore, it can be observed that although the functionalisation works for both materials (PET and PLA) with either treatment, the O_2 plasma treatment followed by EDA immersion displays higher absorbance levels than the NH_3 plasma, for both materials ($p<0.05$). Moreover, while the NH_3 treatment of PET and PLA braids did not display a significant difference (week 1), the EDA treatment displayed significantly lower amino groups grafting values. Both untreated PET and PLA displayed a non-significant Orange II concentration, which is explained by their lack of primary amino groups. On the other hand, all treatment conditions have shown the presence of primary amino groups in their constitution. This method indicates that the method with O_2 plasma followed by immersion in an EDA solution has significantly more primary amino groups [32]. However, it is possible that the NH_3 plasma formed other groups, such as secondary or tertiary amino groups, so further analyses were done.

A qualitative method of detecting the presence of amino groups is the fuchsine method, which gives visual information about the concentration and location of the

amino groups throughout the braids [31]. Thus, the more saturated the purple taint, the more amino groups are present.

This qualitative method is presented in figure 22.

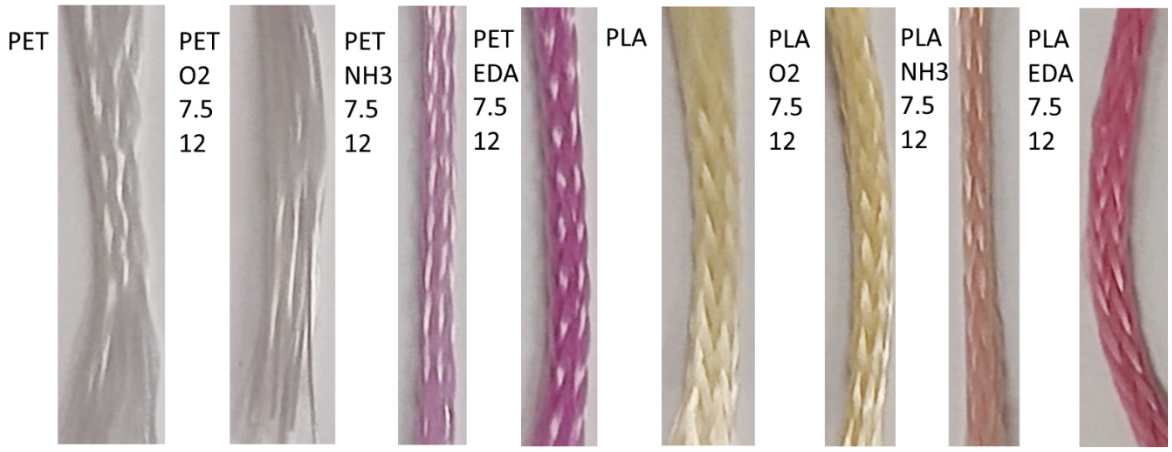


***Figure 22**: Qualitative evaluation of the amino groups' distribution on PET and PLA braids after different treatments.*

By observing figure 22, it can be seen that in both materials, the untreated braid (PET and PLA) are not stained with the purple taint of the fuchsine acid. The same applies to the braids treated with the O_2 plasma, without immersion in the EDA solution.

However, both treated materials, namely the NH_3 plasma-treated braids, as well as the braids immersed in EDA after O_2 plasma exposure, display a very clear and homogeneously distributed purple taint. This means that, in both cases, the treatment was successful, meaning that each braid was homogeneously grafted with amino groups, as intended.

As in the future the braids, once inserted in a more complex hybrid structure, will be implanted *in vivo* and interact with an aqueous medium and cells, a wicking test was performed, presented in figure 23.

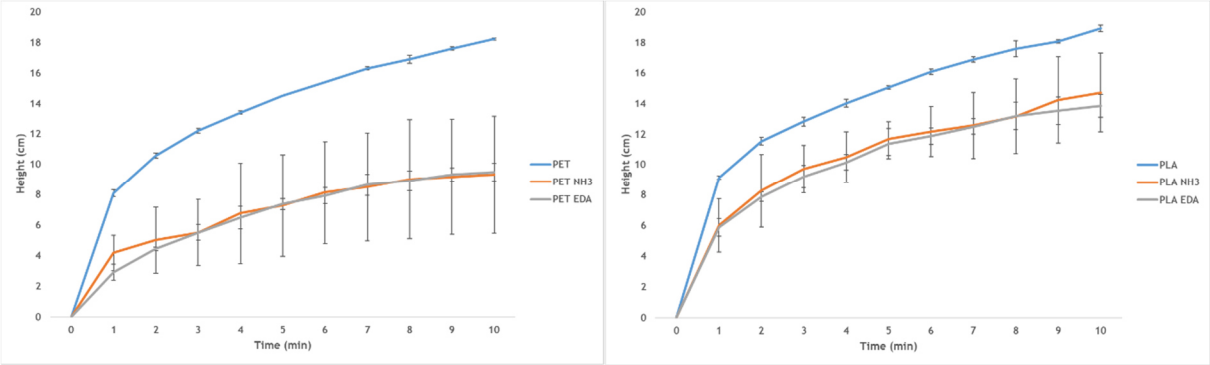


***Figure 23**: Wicking test of PET and PLA braids, for both NH_3 plasma-treated braids and O_2 plasma-treated braids with immersion in EDA.*

While the wicking ability of ammonia and oxygen plasma-treated braids is similar, a wider difference is displayed when compared to the untreated material; this is applied to both PET and PLA braids. This may be explained by the increase of the hydrophilicity of the structure due to the presence of amine groups, which will interact with the water during its rise through the pores throughout the structure. These are adhesion forces, which will lead to the retention of the water in the pores of the structure, thus slowing its rise through the structure.

To observe the topography of the material before and after treatment, SEM images comparing each treatment condition for PET and PLA samples are presented in figure 24 and 25, respectively.

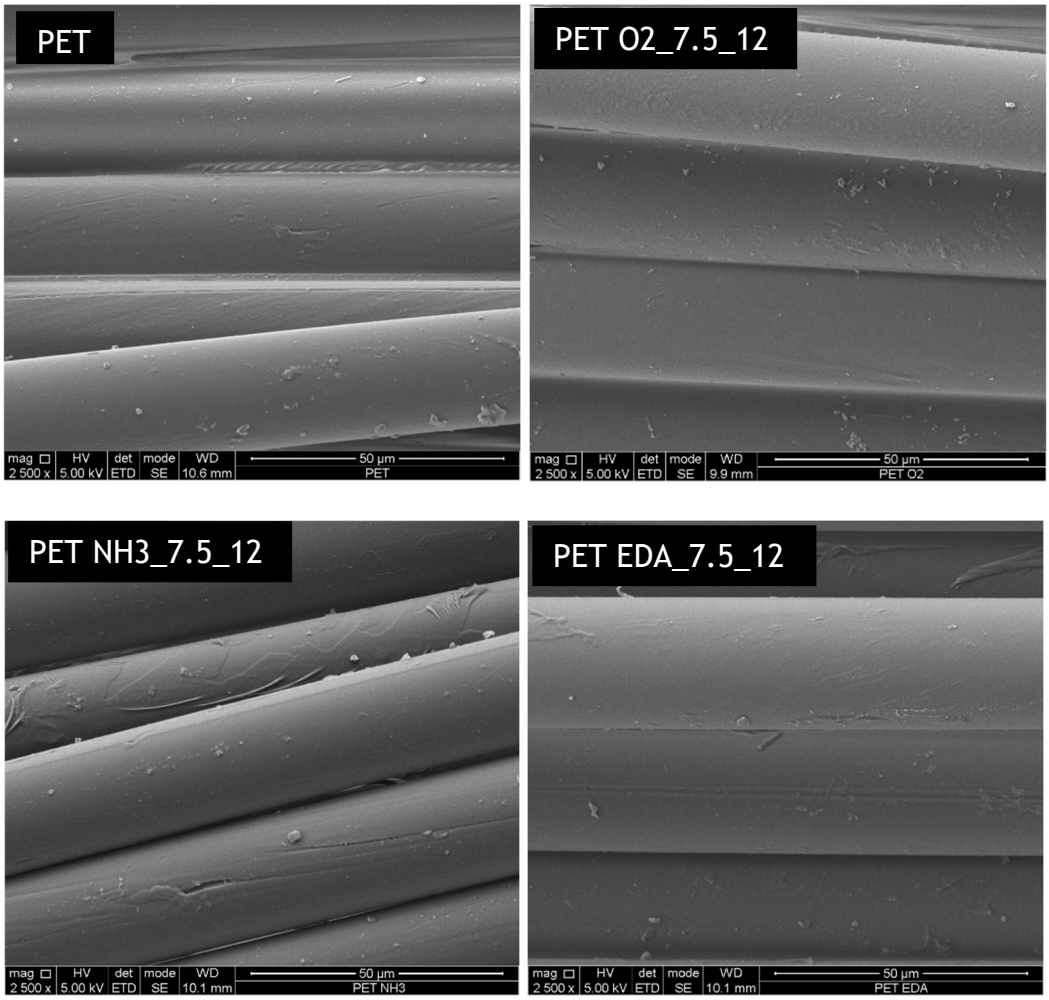


***Figure 24**: SEM images of PET braids, with different treatment conditions.*

In both materials (figure 24 and 25). The O_2 plasma-treated braids seem to have a cleaner surface than the rest. This is because the oxygen plasma may have cleaned some of the impurities present in the braid without damaging the surface [30].

Then, when comparing both the O_2 plasma-treated braids and the braids immersed in EDA afterwards, there are noticeable changes on the surface. These changes are caused by the chemical etching by the EDA solution, in which the braids were immersed for 20 minutes at 50 ºC, and/or by the deposition of the EDA itself.

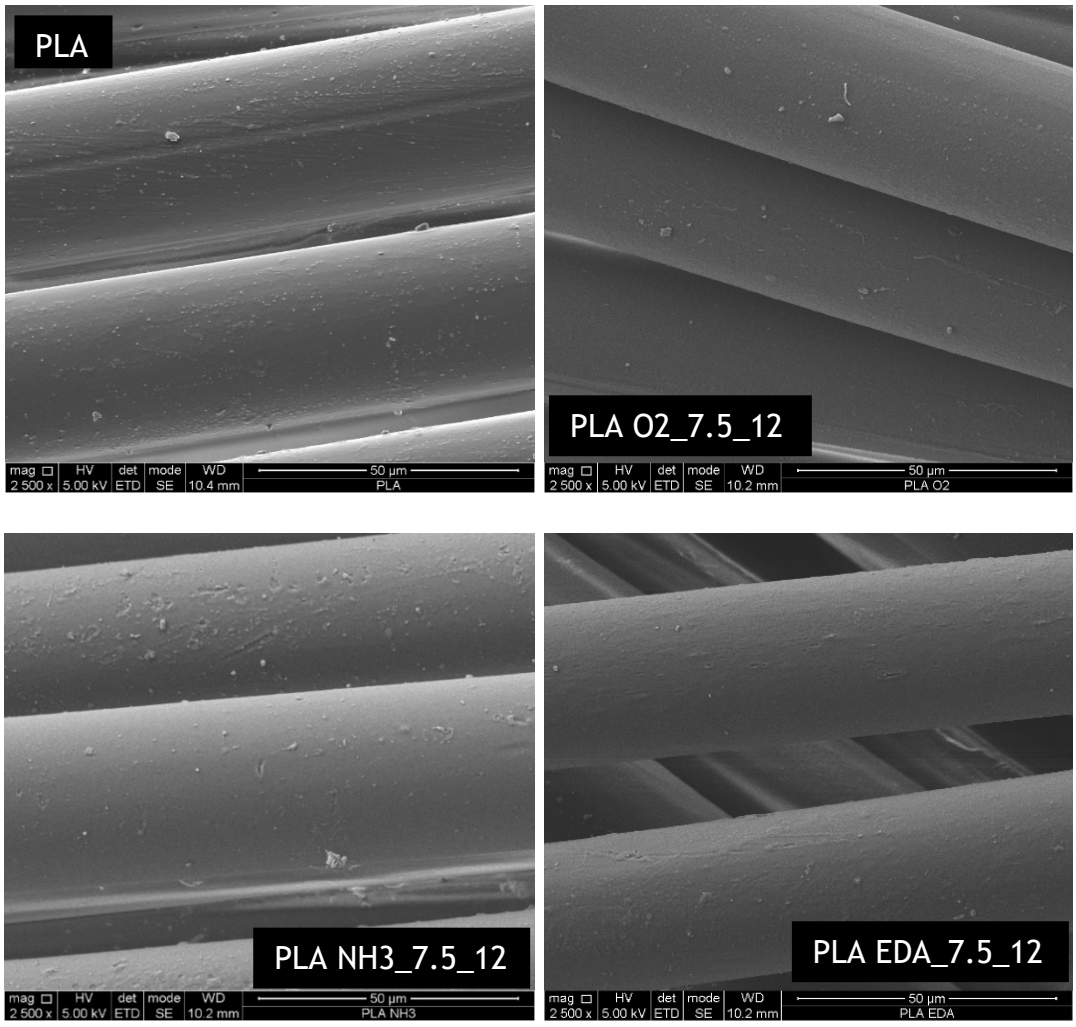


***Figure 25**: SEM images of PLA braids, with different treatment conditions.*

The NH_3 treated braids display more changes in the surface than the rest. As the oxygen plasma-treated braid appears to have a cleaner surface, this is not the case for the ammonia plasma-treated braid. This is to be expected, since the O_2 plasma is already often used for this purpose, so it is better for that than the NH_3 plasma [30]. The applied plasma treatments cause reactions on the polymeric surfaces, since plasma carries activated species which include addition reactions of new functional groups onto the surface, due to a recombination of radicals that are formed on the surface by the activated species in the plasma. Changes in the surface of the polymer surfaces can also be due to the bombardment of the fibre by high energy particles generated in the discharge, as well as surface etching reactions carried by the plasma, which can result in changes in the topography of the surface [35]. Nevertheless, the polymer surfaces were not significantly changed.

An energy dispersive spectroscopy (EDS) analysis was done in order to check the presence of N in the braids. The results are presented in figure 26.

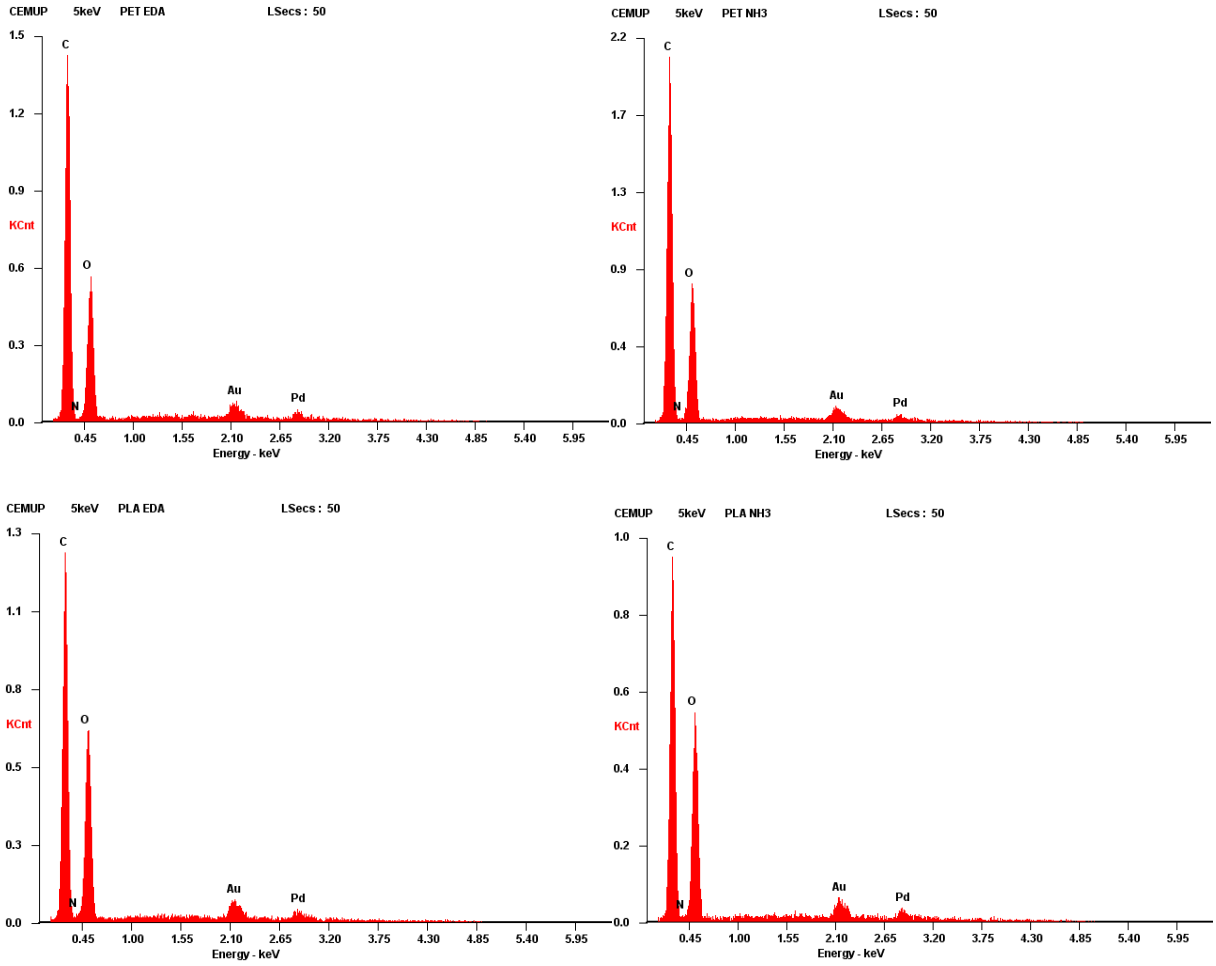


***Figure 26**: EDS scan of treated PET and PLA braids.*

Contrary to what was determined by the Orange II method, no N was found by the EDS analysis. This may be explained by the sensitivity of the technique itself. Therefore, an XPS analysis was done in order to confirm the efficacy of the treatments.

The surface chemical modifications induced by the studied treatments were determined by XPS analysis. By curve-fitting, the C1s, O1s and N1s peaks and chemical bonds on the surface of all samples could be determined. It must be noted that this technique can be used to detect all elements except H and He.

Concerning PET, attending to figure 28 and table 6, the untreated PET samples have an atomic composition of mainly carbon with oxygen, as expected from the chemical composition of this polymer (figure 27): mainly C-C from the benzene ring and C=O, and O-C=O from the ester groups [36].

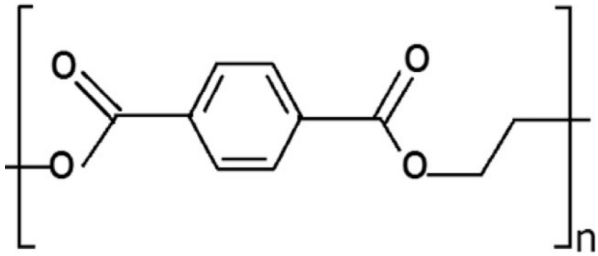


***Figure 27**: Molecular structure of polu(ethylene terephthalate) [37].*

Concerning the NH_3 treated PET braids, attending to table 6, the peaks corresponding to PET are still visible, with small energy shifts due to the clear incorporation of nitrogen on the PET surface, overwhelmingly in the form of primary amines. Secondary amines, amides (N-C=O), and imines (C=N) are also present. Amines, in particular, are known to be very beneficial for initial attachment and later growth of several cell types, with particular emphasis on fibroblasts [38]. This phenomenon was the rationale for the plasma treatment.

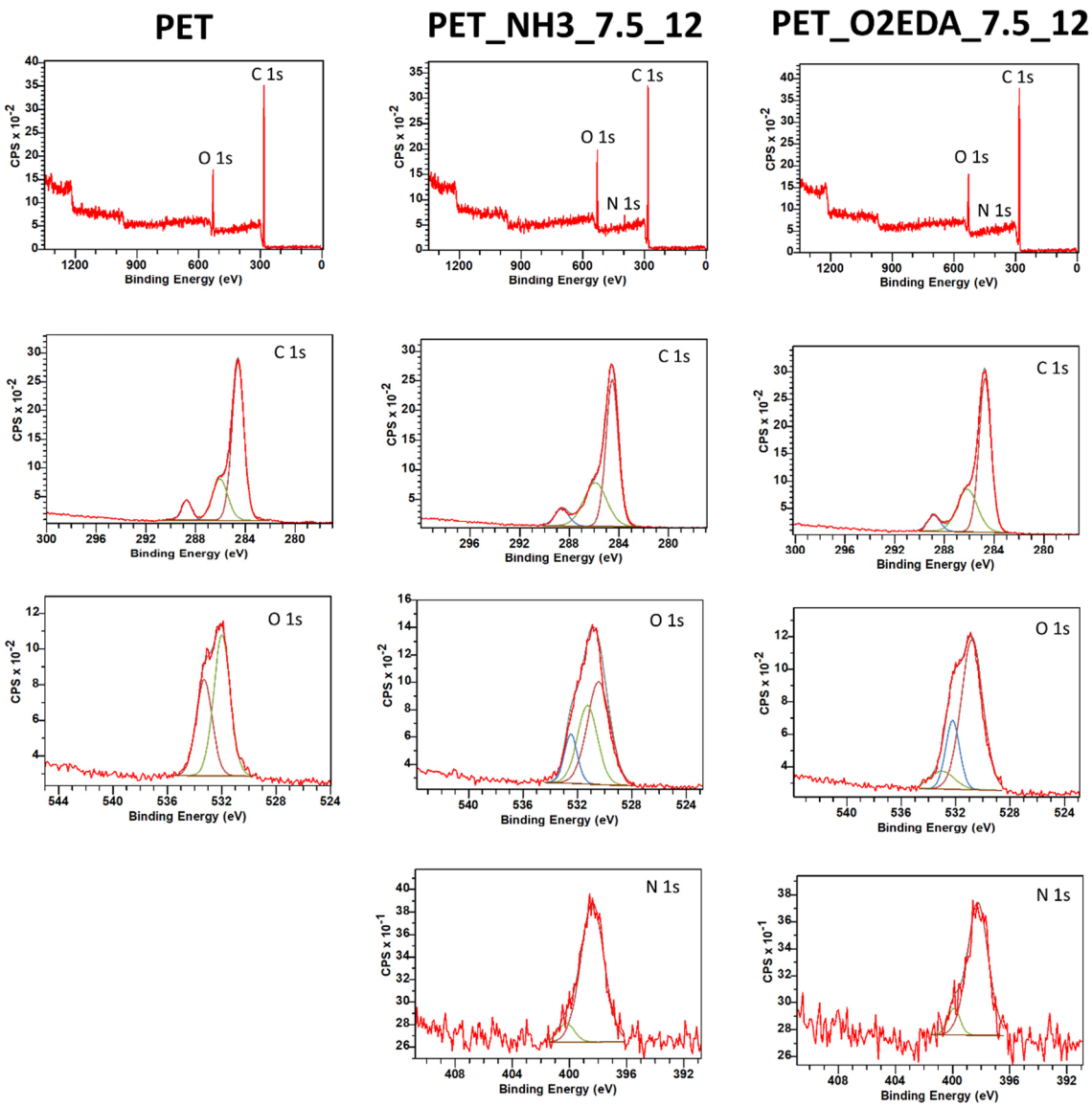


***Figure 28**: XPS overview and detailed spectra of untreated and treated PET braid*

Table 6 also shows the quantitative analysis of PET treated with O_2 plasma followed by EDA grafting. Similarly to the NH_3 plasma treatment, the purpose of endowing the braided structures with amines was accomplished, as seen in the presence of primary amines binding energies (C-NH_2 and C-NH_3^+). When comparing the different plasma treatments on PET (NH_3 and O_2 with immersion in EDA), it is important to mention that the NH_3 plasma displayed a higher atomic concentration of nitrogen, resulting from nitrogen-containing functional groups (mainly primary amines).

***Table 6**: Chemical bonds and binding energy (eV) of PET samples. Bellow each binding energy is atomic concentration (%).*

	C 1s			O 1s			N 1s		
	PET	PET_NH_3	PET_O_2EDA	PET	PET_NH_3	PET_O_2EDA	PET	PET_NH_3	PET_O_2EDA
C-C **C=C**	**284.6** *68.9 %*	**284.6** *59.3 %*	**284.7** *63.3 %*						
C-O **C-N** **C=N**	**286.0** *23.5 %*	**285.9** *32.8 %*	**286.1** *29.8 %*						
O-C=O **N-C=O**	**288.7** *7.5 %*	**288.6** *7.9 %*	**288.9** *6.9 %*						
NH_x-C=O					**530.4** *51.4 %*	**530.8** *69.9 %*			
C=O **N-C=O**				**532.0** *60 %*	**531.3** *34.6 %*	**532.2** *9.5 %*			
C-O **C-O-C** **O-C-O**				**533.3** *40 %*	**532.5** *14.0 %*	**532.9** *20.6 %*			
C-NH_2								**398.4** *91.4 %*	**398.3** *89.7 %*
C-NHR **C=N** **C-NH_3^+**								**400.2** *8.6 %*	**399.0** *10.3 %*

For PLA braids, the analysis of the untreated samples (table 7) showed the expected bonds and binding energies that are typical of this polymer (figure 29), namely C-C and ester (O=C-C) (figure 30). However, after the NH_3 plasma treatment (table 7), along with the previous bonds, nitrogen-containing groups can be detected in the form of amines and imines [39-41].

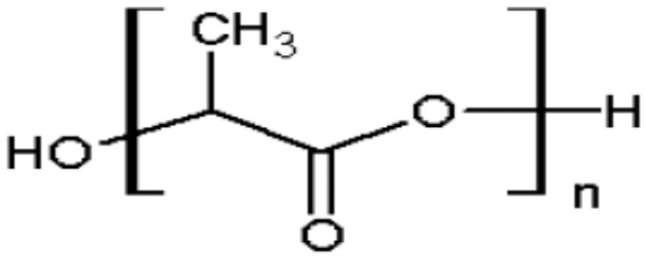


***Figure 29**: Molecular structure of poly(lactide) [42].*

Conversely, for O_2 plasma followed by EDA grafting (table 7), amines and imines are also detectable; however, this treatment yields a much higher concentration of amines when compared with PLA NH_3 plasma-treated samples. This difference corroborates the results obtained by the Orange II and fuchsin acid methods (figures 21 and 22), where there is a significantly higher content of primary amines in the PLA samples with EDA grafting compared to the PLA treated with NH3 plasma.

In all treated samples (for both PET and PLA braids), there was a clear indication of the effective functionalisation with nitrogen-containing groups.

***Table 7**: Chemical bonds and binding energy (eV) of PLA samples. Bellow each binding energy is atomic concentration (%)*

	C 1s			**O 1s**			**N 1s**		
	PLA	PLA_NH_3	PET_O_2EDA	PLA	PLA_NH_3	PET_O_2EDA	PLA	PLA_NH_3	PLA_O_2EDA
C-C **C-H**	**284.6** *68.0 %*	**284.6** *58.5 %*	**284.5** *37.1 %*						
C-O **C-NH2**	**285.9** *26.0 %*	**285.7** *29.2 %*	**286.0** *43.4 %*						
O-C=O **C=O**	**288.9** *6.0 %*	**288.2** *12.3 %*	**288.8** *19.5 %*						
C-O				**531.0** *74.4 %*	**530.8** *60.7 %*	**529.5** *14.7 %*			
C=O				**532.4** *60 %*	**532.2** *39.3 %*	**530.9** *85.3 %*			
C=N								**398.8** *93.3 %*	**397.5** *5.9 %*
C-N								**400.4** *6.7 %*	**398.9** *94.1 %*

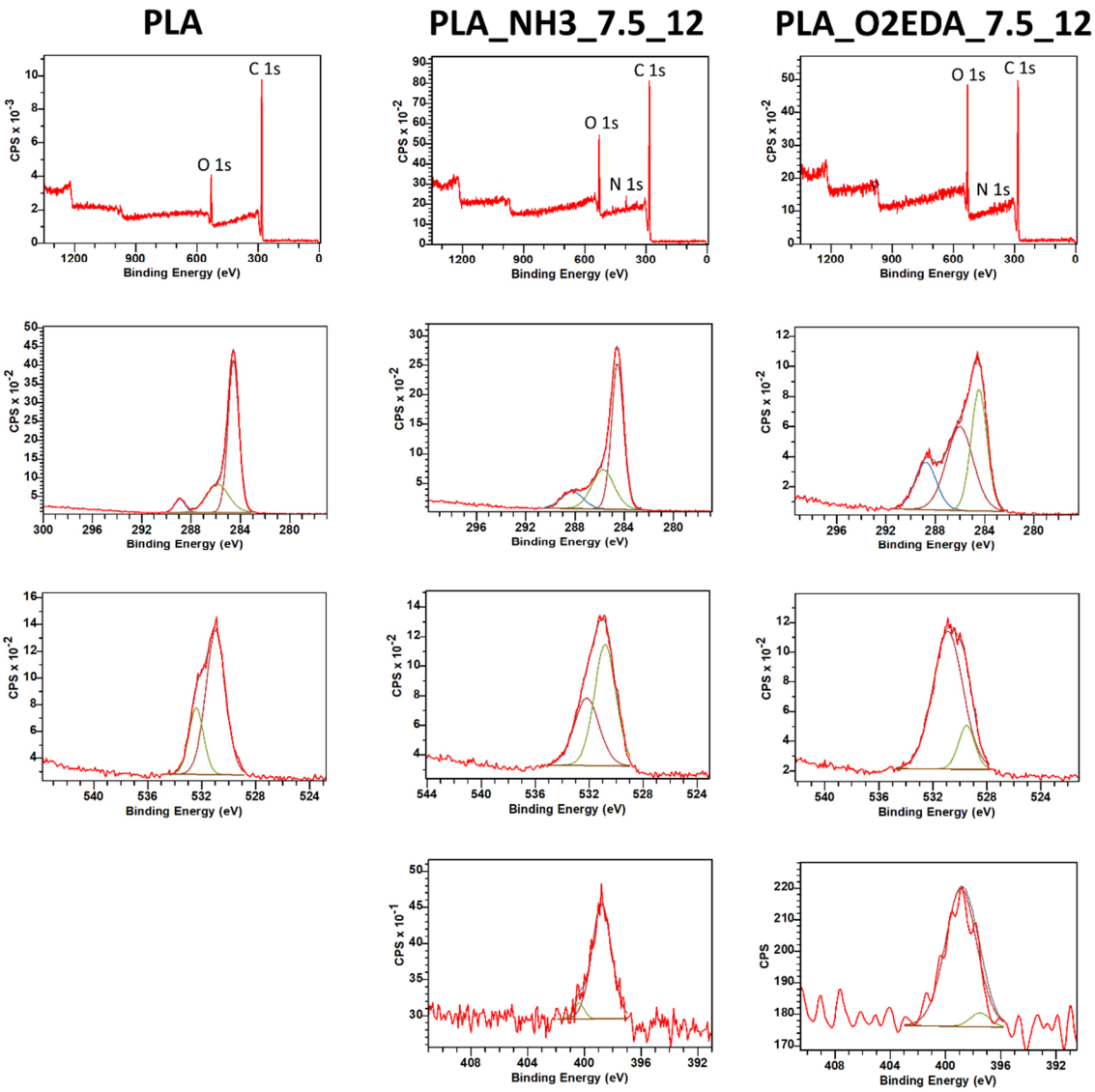


***Figure 30**: XPS overview and detailed spectra of untreated and treated PLA braids.*

4.2. Mechanical behaviour

While PET is a polymer broadly used for its high strength and thermal resistance [35, 43], static tensile tests were performed on the braids treated with the best-determined parameters, namely NH_3 plasma and O_2 plasma, for 12 minutes, the latter followed by immersion in an EDA solution. Braids treated with O_2 plasma without immersion in the EDA solution were also tested in order to test the effect of this immersion on the mechanical performance of the braids. PLA braids were also tested since the final medical device is a hybrid structure composed of both materials (PET

and PLA). The tests were applied on braids of each material in order to evaluate the effect of the treatment on that specific material, and respective differences.

The results of the mechanical testing are presented in figure 31.

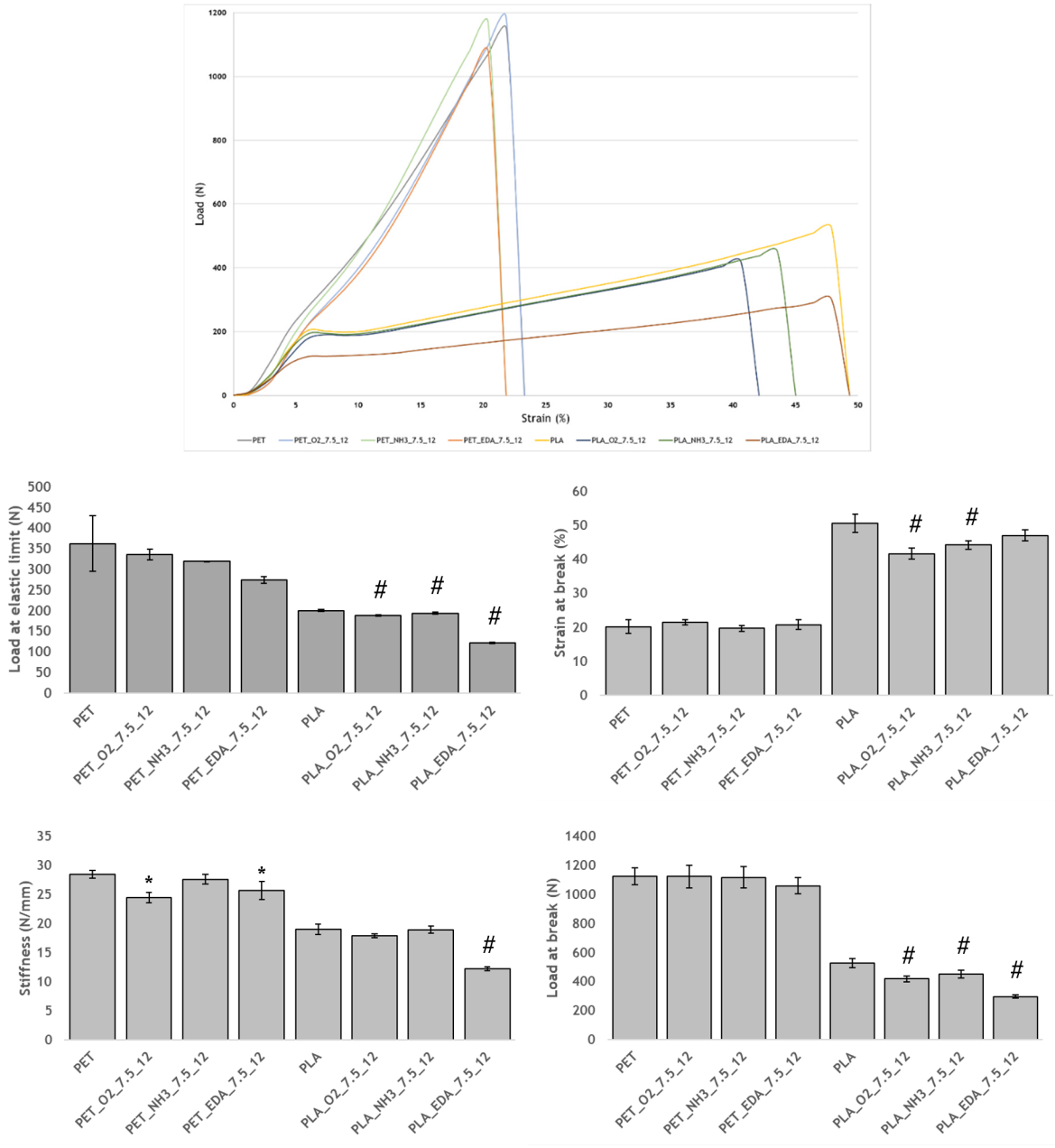


***Figure 31**: Results of the mechanical tests of treated and untreated PET and PLA braids.*

The results show that the treated PET braids show comparable results to the untreated PET braids in all evaluated mechanical properties, with the exception of

stiffness, as the braids treated with O_2 plasma (both immersed in an EDA solution and not) display significantly less ($p<0.05$) stiffness.

On the PLA braids, however, the difference is much more significant, especially on the braid immersed in EDA. All treated PLA braids displayed significantly less ($p<0.05$) load at the elastic limit. While the stiffness was statistically the same in both plasma treatments on PLA fibres when compared to the untreated PLA braids, the braids immersed in EDA displayed significantly less stiffness ($p<0.05$). While the strain at break on the latter was not significantly different when compared to untreated PLA, the load at break of all treated PLA braids was significantly less ($p<0.05$) than the untreated PLA braids. The increased difference in the PLA braids immersed in EDA was most likely caused by hydrolysis, as PLA degrades by hydrolysis and this treatment method requires immersion in an aqueous EDA solution [44]. Another factor to consider is the temperature at which this immersion was performed (50 ºC), which may have increased the degradation on this polymer [45].

The differences in the mechanical behaviour of the treated braids are of most importance in the elastic region: namely, the load at elastic limit and the stiffness, since the final medical device is intended to perform within the elastic region of the final hybrid rope-like structure. As such, a major change in stiffness and load at elastic limit may compromise the mechanical performance of the final rope structure; however, differences were mostly seen on the PLA braids, which will not cause a relevant impact on the rope-like structure due to the fact that it is mechanically supported by the PET braids, and that the PLA will eventually degrade [46].

This structure is mechanically supported by the PET braids [46], so while the stiffness is significantly less in the O_2 plasma-treated braids, the NH_3 plasma-treated braids displayed statistically the same stiffness. Furthermore, none of the treatments on PET braids displayed significantly different results in load at the elastic limit, meaning that the fibre integrity was mostly maintained. It must be noted, though, that the PET braids immersed in an EDA solution after exposure to O_2 plasma have shown significantly less load at the elastic limit when compared to both plasma-treated braids. This difference can be attributed to the additional chemical etching the braids underwent, by the EDA solution.

To summarise, while all treated braids presented comparable results to the untreated PET braids, the NH_3 plasma treatment was the treatment that caused the least changes in the mechanical properties, when compared to the EDA treatment. Furthermore, on the PLA braids, the differences are much more noticeable, especially due to hydrolysis on the EDA immersed braids [44]; however, similarly to the PET braids, the NH_3 plasma treatment caused fewer changes in the mechanical properties, when compared to the EDA treatment.

The final hybrid rope-like structure is intended to temporarily support the mechanical function of the native tissue to allow healing, and this hybrid medical device is mechanically supported by the PET braids [46]. While PLA suffered a loss in mechanical performance, including in the elastic region where the medical device will operate, the final medical device is mechanically supported by the PET braids, meaning that any possible changes in the PET braids are much more relevant to the final application than in PLA braids; the PET braids, however, mostly maintained fibre integrity after treatment. Furthermore, PET braids had fewer changes when treated with the NH_3 plasma, and the changes that occurred in the PLA braids were mostly caused by hydrolysis [44], which occurred while the braids were immersed in an aqueous EDA solution, meaning that, for both materials, the NH_3 plasma treatment method is advantageous when compared to the treatment with the EDA solution.

4.3. *In vitro* biological characterisation

To elucidate the impact of the surface treatments on cell adheasion and proliferation, cell culture assays were performed on PET samples (namely untreated PET, PET treated with NH_3 plasma for 12 minutes, and PET treated with O_2 plasma for 12 minutes, followed by immersion in an aqueous EDA solution) using fibroblasts.

The metabolic activity of the seeded materials was analysed and compared by the resazurin assay over the course of the experiment, at different time points (days 1, 3, 6, 9, 12, 15 and 21). As observed in figure 32, all treated samples display an increase in metabolic activity over time, being the ammonia plasma-treated braids the samples with the most notable growth.

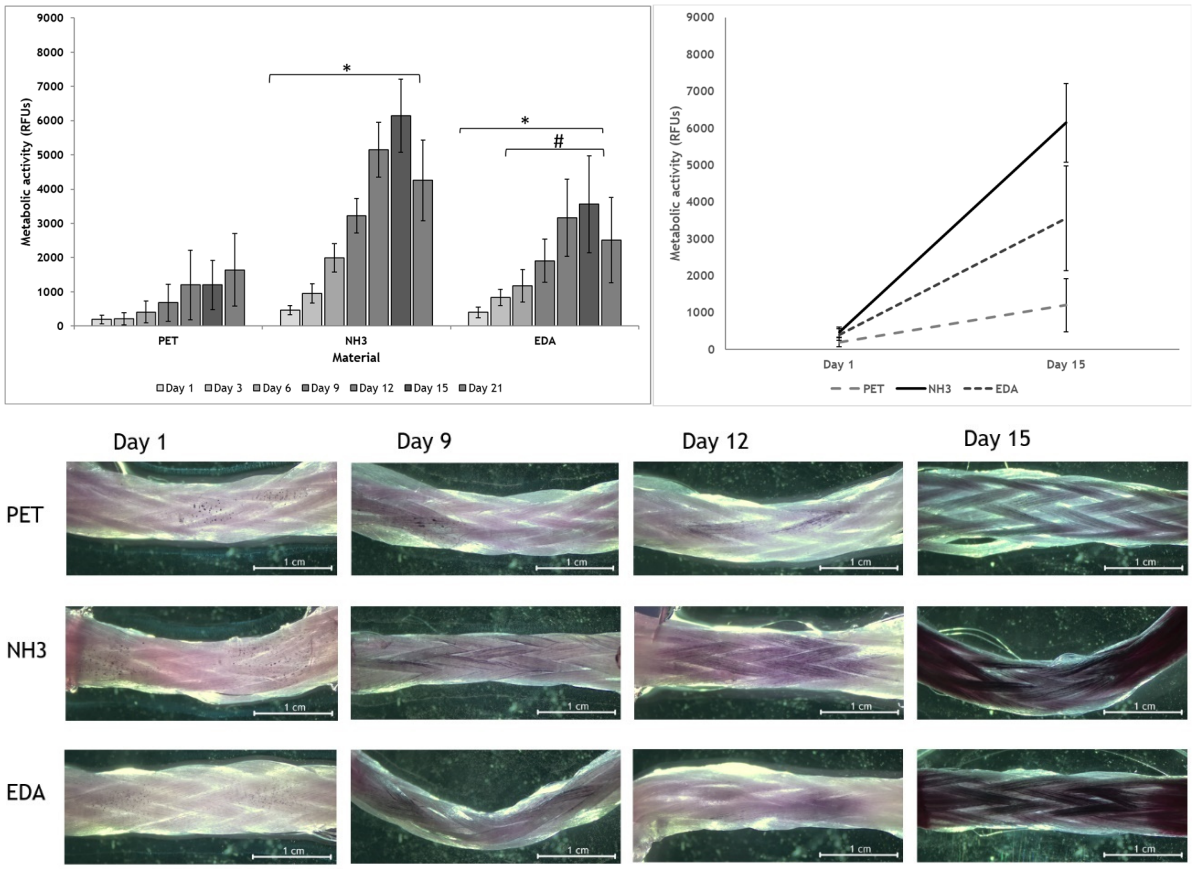


***Figure 32**: A) Metabolic activity of fibroblast cells on PET braids, measured up to 21 days by resazurin assay. *p<0.05, significant differences from PET, for each time-point. #p<0.05, significant differences of EDA from NH_3, for each time-point; B) Growth rate comparing Day 1 to Day 15; C) Microscopic images of fibroblast cells on PET braids, after cells colouring by MTT assay.*

The presence of primary amine groups on polymeric surfaces is of pivotal importance for cell adhesion and proliferation [41]. The goal of both treatments applied to the produced PET braids is to bond the surface with these amine groups, in order to promote cell adhesion and proliferation. As seen from the resazurin assay, as well as the microscopic images, the grafting of the amine groups into the polymer surface does promote, as expected, cell adhesion and proliferation. Furthermore, although both treatments showed significantly more growth compared to the untreated PET braids, the ammonia plasma-treated braids displayed an even more prevalent growth, as seen in figure 32.

It can be concluded that while both treatments promote cell adhesion and proliferation significantly, the ammonia plasma treatment showed better results.

Images of the cells adhering to the surface of the treated PET braids (NH3 plasma and O2 plasma with immersion in EDA) are presented in figure 31.

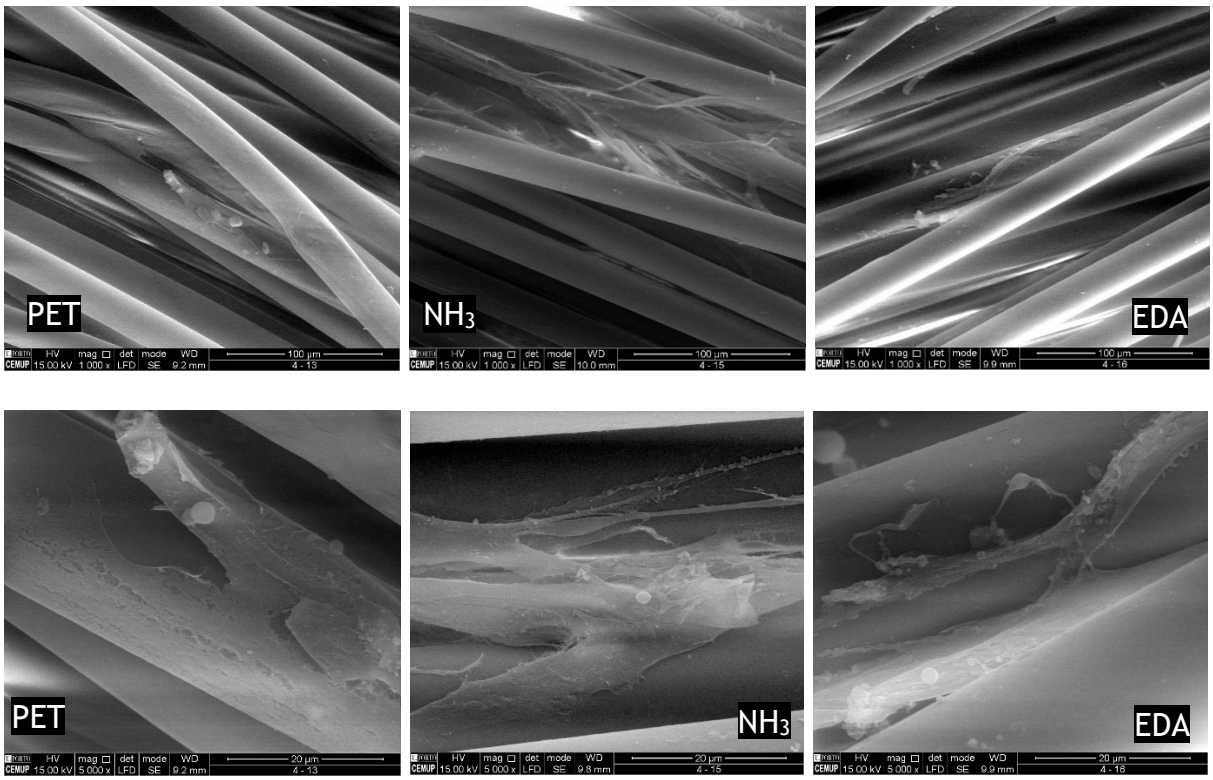


***Figure 33**: SEM images of cell adhesion in PET braids treated with NH3 plasma and O2 plasma followed by immersion in EDA, day 15 of the experiment.*

In figure 33, the dermal fibroblasts can be seen adhering to the structure. These images are of samples taken from the 15th day of the experiment, which was the peak measured in the resazurin assay. From the SEM analysis, it is clear that the seeded cells have migrated to the interior of the braids porous structure and have populated it, which is beneficial having in mind their final application.

The morphology of the seeded human dermal fibroblasts varies in accordance with the type of surface treatment. The cells seeded on the untreated PET fibres displayed adhesion, but were unable to expand the cytoplasm, preventing proliferation and interaction with adjacent fibres. However, the cells seeded on the

EDA treated fibres display an extended morphology with a somewhat restricted interaction with the surrounding fibres. The cell morphology adhering to the NH_3 plasma-treated samples display cytoplasmic spreading with several projections to the surrounding fibres, as depicted in figure 31, meaning that there is strong adhesion to the material, that the cells are well adapted to the material topography, and that there is good interaction within the fibres.

5. Main conclusions and future work

The primary focus of this work was to compare two methods of surface functionalisation of polymeric braided structures for tendon and ligament repair, namely PET and PLA braids, in order to enhance cell adhesion and proliferation.

From the physicochemical characterisation of the treated braids, it was concluded that the purpose of grafting amino groups onto the braids was achieved in both braided materials (PET and PLA) with both the applied treatment methods (NH_3 plasma treatment and O_2 plasma treatment with EDA immersion). It was further observed that while the EDA grafting yielded more primary amino groups, the NH_3 plasma treatment conferred more nitrogen-containing groups.

Concerning the tensile testing performed on the braids, it was concluded that while the PET fibres mostly maintained their mechanical properties, the PLA braids displayed a more considerable loss, especially after immersion in the EDA solution due to hydrolysis. Concerning the overall changes in mechanical properties of each material after each treatment, it was concluded that the NH_3 plasma treatment was advantageous in this field.

Based on the physicochemical and tensile results, the samples treated with a plasma pressure of $7.5*10^{-2}$ mbar for 12 minutes showed the best results.

Regarding the cell culture, the growth rate on the NH_3 plasma-treated braids, as well as the morphology of the cells seeded in these samples, was much more preferable. The observed cytoplasmic spreading and projections to the surrounding fibres show that there is strong adhesion to the material, thus concluding the NH_3 treatment was very successful and achieved the objective of enhancing cell adhesion and proliferation on the material.

Thus, the NH_3 plasma treatment presents clear advantages compared to the usage of O_2 plasma treatment with immersion in an EDA solution. The *in vitro* biological test and the tensile tests both confirmed that the NH_3 plasma treatment is the better alternative for this application. Furthermore, considering the reduced chemical

waste and the fact that it is a one-step process, as the immersion phase is removed, the NH_3 plasma treatment is a more sustainable and easily upscaled process.

Considering the more promising results of the NH_3 plasma treatment on both materials (PET and PLA), the hybrid medical device treated with NH_3 plasma should be *in vivo* tested to evaluate its degradation, mechanical and biological behaviour under conditions similar to the clinical trials.

References

[1] J. Currey, D. Sheng, A. Neph Speciale, C. Cinquini, J. Cuza, and B. L. Waite, "Performing Arts Medicine," *Physical Medicine and Rehabilitation Clinics of North America*, vol. 31, no. 4, pp. 609-632, 2020, doi: https://doi.org/10.1016/j.pmr.2020.08.001. [Online]. Available: http://www.sciencedirect.com/science/article/pii/S1047965120300644

[2] R. W. Dick, J. R. Berning, W. Dawson, R. D. Ginsburg, C. Miller, and G. T. Shybut, "Athletes and the Arts — The Role of Sports Medicine in the Performing Arts," *Current Sports Medicine Reports*, vol. 12, no. 6, 2013. [Online]. Available: https://journals.lww.com/acsm-csmr/Fulltext/2013/11000/Athletes_and_the_Arts___The_Role_of_Sports.12.aspx

[3] F. J. Bejjani, G. M. Kaye, and M. Benham, "Musculoskeletal and neuromuscular conditions of instrumental musicians," *Archives of Physical Medicine and Rehabilitation*, vol. 77, no. 4, pp. 406-413, 1996, doi: https://doi.org/10.1016/S0003-9993(96)90093-3. [Online]. Available: http://www.sciencedirect.com/science/article/pii/S0003999396900933

[4] K. Intziegianni, "Influence of age and pathology on Achilles tendon properties under functional tasks," 2017.

[5] T. Peixoto, M. C. Paiva, A. T. Marques, and M. A. Lopes, "Potential of Graphene–Polymer Composites for Ligament and Tendon Repair: A Review," *Advanced Engineering Materials*, vol. n/a, no. n/a, p. 2000492, 2020, doi: 10.1002/adem.202000492. [Online]. Available: https://doi.org/10.1002/adem.202000492. Accessed: 2020/10/29.

[6] D. S. Morais, J. Torres, R. M. Guedes, and M. A. Lopes, "Current Approaches and Future Trends to Promote Tendon Repair," *Annals of Biomedical Engineering*, vol. 43, no. 9, pp. 2025-2035, 2015, doi: 10.1007/s10439-015-1369-5. [Online]. Available: https://doi.org/10.1007/s10439-015-1369-5

[7] K. Parmar, "Tendon and ligament: basic science, injury and repair," *Orthopaedics and Trauma*, vol. 32, no. 4, pp. 241-244, 2018, doi: 10.1016/j.mporth.2018.05.008.

[8] B. H. Hodgens, J. S. Geller, M. G. Rizzo, J. Munoz, J. Kaplan, and A. Aiyer, "Performance Outcomes After Surgical Repair of Achilles Tendon Rupture in the Women's National Basketball Association," *Orthopaedic Journal of Sports Medicine*, vol. 9, no. 9, p. 23259671211030473, 2021, doi: 10.1177/23259671211030473. [Online]. Available: https://doi.org/10.1177/23259671211030473. Accessed: 2021/11/04.

[9] A. Chauhan, J. Stotts, O. R. Ayeni, and M. Khan, "Return to play, performance, and value of National Basketball Association players following Achilles tendon rupture," *The Physician and Sportsmedicine*, vol. 49, no. 3, pp. 271-277, 2021, doi: 10.1080/00913847.2021.1932634. [Online]. Available: https://doi.org/10.1080/00913847.2021.1932634

[10] M. L. Killian, L. Cavinatto, L. M. Galatz, and S. Thomopoulos, "The role of mechanobiology in tendon healing," *Journal of Shoulder and Elbow Surgery*, vol. 21, no. 2, pp. 228-237, 2012, doi: https://doi.org/10.1016/j.jse.2011.11.002. [Online]. Available: http://www.sciencedirect.com/science/article/pii/S1058274611005611

[11] M. Benjamin, T. Kumai, S. Milz, B. M. Boszczyk, A. A. Boszczyk, and J. R. Ralphs, "The skeletal attachment of tendons—tendon 'entheses'," *Comparative Biochemistry and Physiology Part A: Molecular & Integrative Physiology*, vol. 133, no. 4, pp. 931-945, 2002, doi: https://doi.org/10.1016/S1095-6433(02)00138-1. [Online]. Available: http://www.sciencedirect.com/science/article/pii/S1095643302001381

[12] D. McGonagle and M. Benjamin. https://enthesis.info/anatomy/muscle_and_enthesis.html (accessed 02 January 2021).

[13] M. Marieswaran, I. Jain, B. Garg, V. Sharma, and D. Kalyanasundaram, "A Review on Biomechanics of Anterior Cruciate Ligament and Materials for Reconstruction," *Appl Bionics Biomech*, vol. 2018, p. 4657824, 2018, doi: 10.1155/2018/4657824.

[14] J. H. C. Wang, "Mechanobiology of tendon," *Journal of Biomechanics*, vol. 39, no. 9, pp. 1563-1582, 2006, doi: https://doi.org/10.1016/j.jbiomech.2005.05.011. [Online]. Available: http://www.sciencedirect.com/science/article/pii/S0021929005002265

[15] A. Sensini and L. Cristofolini, "Biofabrication of Electrospun Scaffolds for the Regeneration of Tendons and Ligaments," *Materials*, vol. 11, p. 1963, 2018, doi: 10.3390/ma11101963.

[16] M. N. Doral *et al.*, "Functional anatomy of the Achilles tendon," *Knee Surgery, Sports Traumatology, Arthroscopy*, vol. 18, no. 5, pp. 638-643, 2010, doi: 10.1007/s00167-010-1083-7. [Online]. Available: https://doi.org/10.1007/s00167-010-1083-7

[17] F. R. Noyes and E. S. Grood, "The strength of the anterior cruciate ligament in humans and Rhesus monkeys," *J Bone Joint Surg Am*, vol. 58, no. 8, pp. 1074-82, 1976.

[18] I. Lindemann, B. K. Coombes, K. Tucker, F. Hug, and T. J. M. Dick, "Age-related differences in gastrocnemii muscles and Achilles tendon mechanical properties in vivo," *Journal of Biomechanics*, vol. 112, p. 110067, 2020, doi: https://doi.org/10.1016/j.jbiomech.2020.110067. [Online]. Available: http://www.sciencedirect.com/science/article/pii/S0021929020304917

[19] G. Walden, X. Liao, S. Donell, M. Raxworthy, G. Riley, and A. Saeed, "A Clinical, Biological and Biomaterials Perspective into Tendon Injuries and Regeneration," *Tissue Engineering Part B: Reviews*, vol. 23, 2016, doi: 10.1089/ten.TEB.2016.0181.

[20] A. E. C. Nichols, K. T. Best, and A. E. Loiselle, "The cellular basis of fibrotic tendon healing: challenges and opportunities," *Translational Research*, vol. 209, pp. 156-168, 2019, doi: https://doi.org/10.1016/j.trsl.2019.02.002. [Online]. Available: http://www.sciencedirect.com/science/article/pii/S1931524419300246

[21] Stryker. "TissueMend." https://www.stryker.com/us/en/sports-medicine/products/tissuemend.html

[22] U. D'Amora, A. Gloria, and L. Ambrosio, "10 - Composite materials for ligaments and tendons replacement," in *Biomedical Composites (Second Edition)*, L. Ambrosio, Ed.: Woodhead Publishing, 2017, pp. 215-235, doi: https://doi.org/10.1016/B978-0-08-100752-5.00010-X. [Online]. Available: http://www.sciencedirect.com/science/article/pii/B978008100752500010X

[23] Neoligaments. "Leeds Kuff-Patch." https://www.neoligaments.com/product/leeds-kuff-patch/ (accessed January 02, 2021).

[24] L. Ligament. "Lars Ligament." https://www.lars-ligaments.com/ (accessed January 02, 2020).

[25] Y. E. Elmogahzy, "16 - Performance characteristics of technical textiles: Part III: Healthcare and protective textiles," in *Engineering Textiles (Second Edition)*, Y. E. Elmogahzy, Ed.: Woodhead Publishing, 2020, pp. 399-432, doi: https://doi.org/10.1016/B978-0-08-102488-1.00016-2. [Online]. Available: http://www.sciencedirect.com/science/article/pii/B9780081024881000162

[26] D. S. Morais, J. Cruz, R. Fangueiro, H. Lopes, R. M. Guedes, and M. A. Lopes, "Mechanical behavior of ropes based on polypropylene (PP) and poly(ethylene terephthalate) (PET) multifilament yarns for Achilles tendon partial substitution," *Journal of the Mechanical Behavior of Biomedical Materials*, vol. 106, p. 103734, 2020, doi: https://doi.org/10.1016/j.jmbbm.2020.103734. [Online]. Available: http://www.sciencedirect.com/science/article/pii/S1751616120302885

[27] D. S. Morais, J. Cruz, R. Fangueiro, M. A. Lopes, and R. M. Guedes, "Characterization of polypropylene (PP) and poly(ethylene terephthalate) (PET) multifilament braided textile structures for Achilles tendon partial substitution," *Mechanics of Materials*, vol. 153, p. 103668, 2021, doi: https://doi.org/10.1016/j.mechmat.2020.103668. [Online]. Available: https://www.sciencedirect.com/science/article/pii/S0167663620307018

[28] C. Jiang, K. Wang, Y. Liu, C. Zhang, and B. Wang, "Application of textile technology in tissue engineering: A review," *Acta Biomaterialia*, vol. 128, pp. 60-76, 2021, doi: https://doi.org/10.1016/j.actbio.2021.04.047. [Online]. Available: https://www.sciencedirect.com/science/article/pii/S1742706121002932

[29] A. Vesel, M. Mozetic, and A. Zalar, "XPS study of oxygen plasma activated PET," *Vacuum*, vol. 82, no. 2, pp. 248-251, 2007, doi: https://doi.org/10.1016/j.vacuum.2007.07.021. [Online]. Available: https://www.sciencedirect.com/science/article/pii/S0042207X07002394

[30] C. M. Chan, T. M. Ko, and H. Hiraoka, "Polymer surface modification by plasmas and photons," *Surface Science Reports*, vol. 24, no. 1, pp. 1-54, 1996, doi: https://doi.org/10.1016/0167-5729(96)80003-3. [Online]. Available: https://www.sciencedirect.com/science/article/pii/0167572996800033

[31] D. Santos Morais *et al.*, "Bioactive and biopassive treatment of poly(ethylene terephthalate) multifilament textile yarns to improve/prevent fibroblast viability," *Journal of Biomedical Materials Research Part B: Applied Biomaterials*, vol. 109, no. 12, pp. 2213-2226, 2021, doi: https://doi.org/10.1002/jbm.b.34882. [Online]. Available: https://onlinelibrary.wiley.com/doi/abs/10.1002/jbm.b.34882

[32] S. Noel, B. Liberelle, L. Robitaille, and G. De Crescenzo, "Quantification of Primary Amine Groups Available for Subsequent Biofunctionalization of Polymer Surfaces," *Bioconjugate Chemistry*, vol. 22, no. 8, pp. 1690-1699, 2011, doi: 10.1021/bc200259c. [Online]. Available: https://doi.org/10.1021/bc200259c

[33] Q. Cheng, B. L.-P. Lee, K. Komvopoulos, Z. Yan, and S. Li, "Plasma surface chemical treatment of electrospun poly(L-lactide) microfibrous scaffolds for enhanced cell adhesion, growth, and infiltration," *Tissue engineering. Part A*, vol. 19, no. 9-10, pp. 1188-1198, 2013, doi: 10.1089/ten.TEA.2011.0725. [Online]. Available: https://pubmed.ncbi.nlm.nih.gov/23281641

https://www.ncbi.nlm.nih.gov/pmc/articles/PMC3609642/

[34] J. Casimiro, B. Lepoittevin, P. Jegou, and P. Roger, "2 3 Introduction of Primary Amino Groups on Poly(ethylene terephthalate) Surfaces by Ammonia and a Mix of Nitrogen and Hydrogen Plasma," *Plasma Chemistry and Plasma Processing*, vol. 32, 2012, doi: 10.1007/s11090-011-9345-9.

[35] N. Inagaki, K. Narushim, N. Tuchida, and K. Miyazaki, "Surface characterization of plasma-modified poly(ethylene terephthalate) film surfaces," *Journal of Polymer Science Part B: Polymer Physics*, vol. 42, no. 20, pp. 3727-3740, 2004, doi: https://doi.org/10.1002/polb.20234. [Online]. Available: https://onlinelibrary.wiley.com/doi/abs/10.1002/polb.20234

[36] M. Gorjanc *et al.*, "Plasma treated polyethylene terephthalate for increased embedment of UV-responsive microcapsules," *Applied Surface Science*, vol. 419, pp. 224-234, 2017, doi: https://doi.org/10.1016/j.apsusc.2017.04.177.

[Online]. Available: https://www.sciencedirect.com/science/article/pii/S0169433217312126

[37] G. Lu *et al.*, "Degradation of Microcellular PET reflective materials used in LED-based products," ed, 2016.

[38] P. Černochová *et al.*, "Cell type specific adhesion to surfaces functionalised by amine plasma polymers," *Scientific Reports*, vol. 10, no. 1, p. 9357, 2020, doi: 10.1038/s41598-020-65889-y. [Online]. Available: https://doi.org/10.1038/s41598-020-65889-y

[39] J. Casimiro *et al.*, "Introduction of Primary Amino Groups on Poly(ethylene terephthalate) Surfaces by Ammonia and a Mix of Nitrogen and Hydrogen Plasma," *Plasma Chemistry and Plasma Processing*, vol. 32, no. 2, pp. 305-323, 2012, doi: 10.1007/s11090-011-9345-9. [Online]. Available: https://doi.org/10.1007/s11090-011-9345-9

[40] Z. Zheng, L. Ren, Z. Zhai, Y. Wang, and F. Hang, "Surface modification on polyethylene terephthalate films with 2-methacryloyloxyethyl phosphorylcholine," *Materials Science and Engineering: C*, vol. 33, no. 5, pp. 3041-3046, 2013, doi: https://doi.org/10.1016/j.msec.2013.03.036. [Online]. Available: https://www.sciencedirect.com/science/article/pii/S0928493113001987

[41] E. Rodríguez-Alba *et al.*, "Surface modification of polyethylenterephthalate film with primary amines using gamma radiation and aminolysis reaction for cell adhesion studies," *Radiation Physics and Chemistry*, vol. 176, p. 109070, 2020, doi: https://doi.org/10.1016/j.radphyschem.2020.109070. [Online]. Available: https://www.sciencedirect.com/science/article/pii/S0969806X20304539

[42] A. Mahapatro and D. Singh, "Biodegradable Nanoparticles are Excellent Vehicle for Site Directed in-vivo Delivery of Drugs and Vaccines," *Journal of nanobiotechnology*, vol. 9, p. 55, 2011, doi: 10.1186/1477-3155-9-55.

[43] A. M. Grumezescu *et al.*, "Electrospun Polyethylene Terephthalate Nanofibers Loaded with Silver Nanoparticles: Novel Approach in Anti-Infective Therapy," *J Clin Med*, vol. 8, no. 7, 2019, doi: 10.3390/jcm8071039.

[44] E. J. Rodriguez, B. Marcos, and M. A. Huneault, "Hydrolysis of polylactide in aqueous media," *Journal of Applied Polymer Science*, vol. 133, no. 44, 2016,

doi: https://doi.org/10.1002/app.44152. [Online]. Available: https://doi.org/10.1002/app.44152. Accessed: 2022/03/27.

[45] M. K. Mitchell and D. E. Hirt, "Degradation of PLA fibers at elevated temperature and humidity," *Polymer Engineering & Science*, vol. 55, no. 7, pp. 1652-1660, 2015, doi: https://doi.org/10.1002/pen.24003. [Online]. Available: https://onlinelibrary.wiley.com/doi/abs/10.1002/pen.24003

[46] T. Peixoto, S. Carneiro, R. Fangueiro, R. M. Guedes, M. C. Paiva, and M. A. Lopes, "Engineering hybrid textile braids for tendon and ligament repair application," *Journal of Applied Polymer Science*, vol. n/a, no. n/a, p. 52013, doi: https://doi.org/10.1002/app.52013. [Online]. Available: https://onlinelibrary.wiley.com/doi/abs/10.1002/app.52013